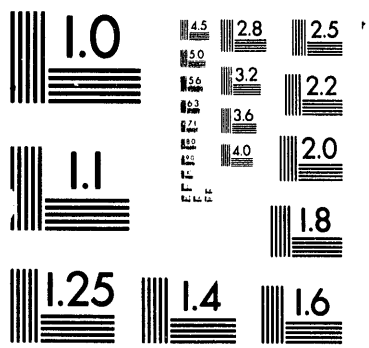
1.0
1.1
1.25
1.4
1.6
1.8
2.0
2.2
2.5
2.8
3.2
3.6
4.0
4.5
5.0
5.6
6.3
7.1
8.0
9.0

1 of 1

# *IN SITU* GAMMA-RAY SPECTROMETRY -- A TUTORIAL FOR ENVIRONMENTAL RADIATION SCIENTISTS

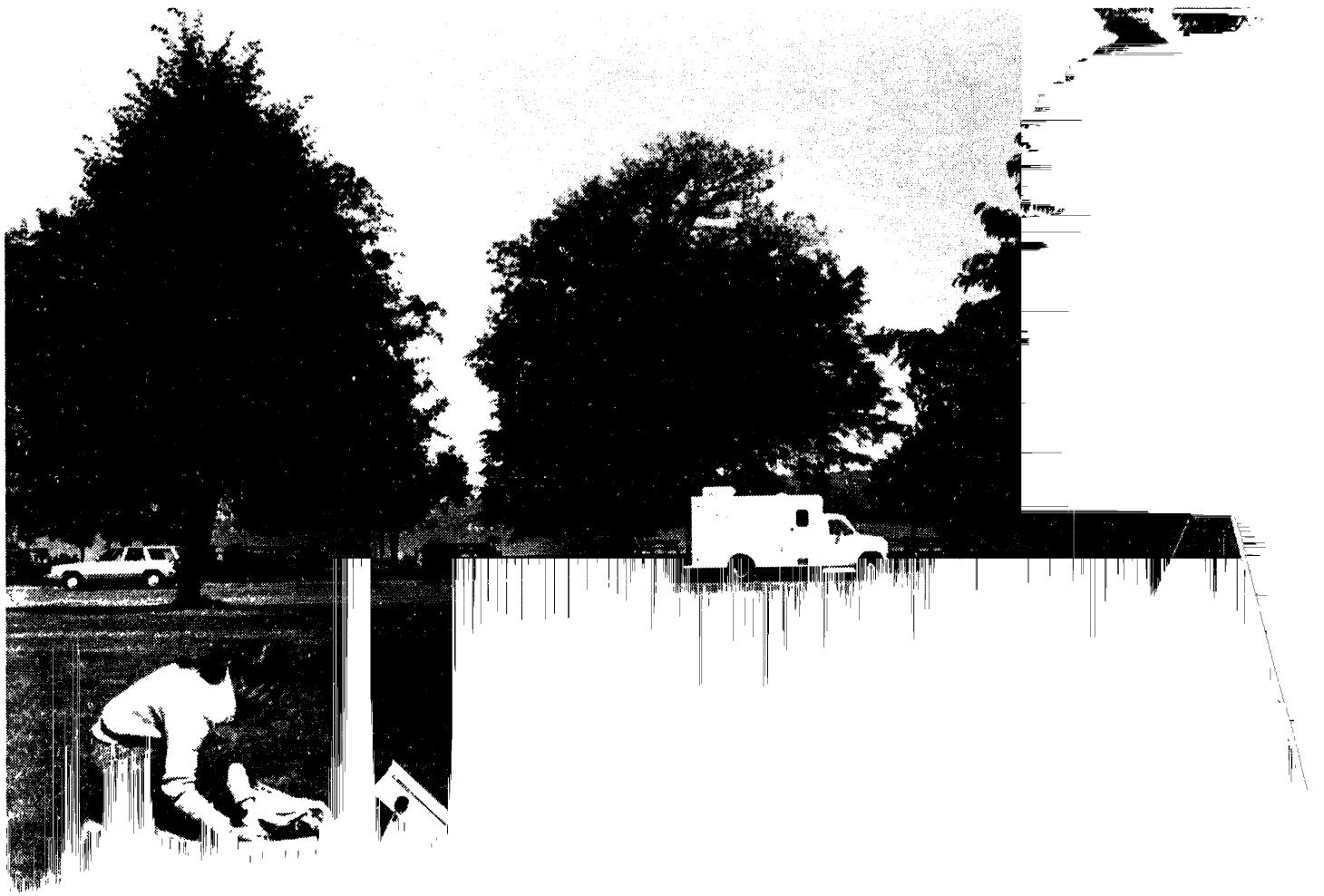

## *ERRATA*

Page 6, par. 1, line 5: units of $S_o$ "(photon/cm$^2$-sec)" should be "(photon/cm$^3$-sec)"

Page 10, par. 1, line 2: "$(\alpha/\rho)/(\rho/\mu_s)$" shoud be "$(\alpha/\rho)\cdot(\rho/\mu_s)$"

Page 17, par. 3, line 6: "value of r" should be "value of x"

Page 17, par. 4, line 1: "value of r" should be "value of x"

Page 24, Equation (3.2): term in front of integral sign "$1/\rho$" should be "$1/\Phi$"

Page 34, last line: "$N_f/A + I/A$" should be "$N_f/A \div I/A$"

EML-557

# *IN SITU* GAMMA-RAY SPECTROMETRY

## *A TUTORIAL FOR ENVIRONMENTAL RADIATION SCIENTISTS*

Kevin M. Miller and Peter Shebell

**Environmental Measurements Laboratory**
**U. S. Department of Energy**
**New York, NY 10014-3621**

**October 1993**

## DISCLAIMER

## ABSTRACT

This tutorial is intended for those in the environmental field who perform assessments in areas where there is radioactive contamination in the surface soil. Techniques will be introduced for performing on-site quantitative measurements of gamma radiation in the environment using high resolution germanium detectors. A basic understanding of ionizing radiation principles is assumed; however, a detailed knowledge of gamma spectrometry systems is not required. Emphasized is the practical end of operations in the field and the conversion of measured full absorption peak count rates in a collected spectrum to meaningful radiological quantities, such as the concentration of a radionuclide in the soil, activity per unit area, and dose rate in the air. The theory of operation and calibration procedures will be covered in detail to provide the necessary knowledge to adapt the technique to site-specific problems. Example calculations for detector calibration are also provided.

## FOREWORD

Most of us who deal with aspects of ionizing radiation in the environment are familiar with basic dose rate measurements using survey instruments. Perhaps we can recall those times where we have walked about a site with a meter in our hand and measured external radiation levels. This constitutes an *in situ* measurement in its most basic form, one which deals with a single parameter such as the exposure rate. For more information, one can take a sample from this same site, perhaps soil, and return it to the laboratory for analysis. Gamma-ray counting on a germanium (Ge) detector might then be employed to determine the specific radionuclides present in the sample. This could be done for strictly qualitative purposes or perhaps to convert measured concentrations of radionuclides in the samples to the exposure rate at the original site using conversion factors. The technique of *in situ* spectrometry combines elements of both of these methods for characterizing the external radiation field. By using a high resolution Ge spectrometer placed over the ground, a spectrum of gamma radiation collected in the field can be used to identify radionuclides present in a qualitative manner by simply looking for the presence of peaks at characteristic energies. At a higher level of sophistication, one can convert the measured peak count rate into some more meaningful quantity such as the concentration of these nuclides in the soil or, in the case of deposited fallout, the activity per unit area. It is also possible to infer the contribution of each individual nuclide to the dose rate in air. This tutorial will introduce you to these techniques, known as "*in situ* gamma-ray spectrometry". A generalized approach is taken so that the individual will be able to adapt the technique to unique situations. To this end, a basic grounding in the theory is given, however short-cut methods are also presented for those who may use the technique for approximate measurements. For more detail on certain aspects, appropriate references are given.

# INTRODUCTION

The term *in situ* is taken from Latin and translates to "in the original place". Thus, given a site where radioactivity and radiation levels are under investigation, the term "*in situ* gamma-ray spectrometry" implies that a spectrum of the ambient gamma-ray flux would be collected at the site and analyzed, principally to identify and quantify the radionuclides present. Sometimes, a less academic term is used, i.e., "field gamma-ray spectrometry," which implying that one is in the outdoor environment.

The technique of *in situ* spectrometry had its origins during the time of atmospheric nuclear weapons testing where it was found to provide quick, reliable information on the components of the outdoor radiation environment. It provided a means to separate natural background from man-made sources and give quantitative results. Over the years, it has been employed by various groups for assessing radiation sources in the environment not only via ground based detectors, but with aircraft systems as well. It proved particularly useful following the Chernobyl accident and was employed by a number of European laboratories. It should prove adaptable to site assessments in the current era of environmental restoration.

The power in the technique of *in situ* spectrometry lies in the fact that a detector placed over a ground surface measures gamma radiation from sources over an area of several hundred square meters. As an example of the effective ground area being measured by a detector at 1 m above the ground, Figure I.1 shows the relative contribution to the fluence from different rings of ground area about the detector for a typical source of fallout $^{137}Cs$ (gamma energy of 662 keV) in the environment. The "field of view" for the detector would be larger for higher energy sources and for sources closer to the soil surface. In contrast, a soil sample would represent an area of but a few tens or hundreds of square centimeters. In practice, an effective characterization of a site would involve *in situ* spectrometry in conjunction with soil sampling. As part of an overall program, *in situ* spectrometry provides a means to assess the degree of contamination in areas during the course of operations in the field, thus guiding the investigator on where to collect samples. It can also substantially reduce the number of samples that need to be collected and subsequently analyzed.

Some of the limitations of *in situ* spectrometry need to be pointed out from the start. Due to the nature of radiation transport through matter (the soil and air), it is for the most part limited to the measurement of gamma and, to some extent, x-ray emitters. Even so, the attenuation properties of soil are such that buried sources are not likely to be detected with measurements performed above ground. At 662 keV, 30 cm of soil will cut out about 97% of the primary flux from a buried point source. Of course, a detector can be lowered into a bore hole for measuring a buried source and techniques applied for interpreting a collected spectrum. While this constitutes an *in situ* measurement in the broad sense of the term, it will not be addressed in this tutorial. We will instead limit the subject area to measurements performed near ground level, where the distribution of the source is expected to be spread out over a fairly large area and where the source is at or near the surface of the soil.

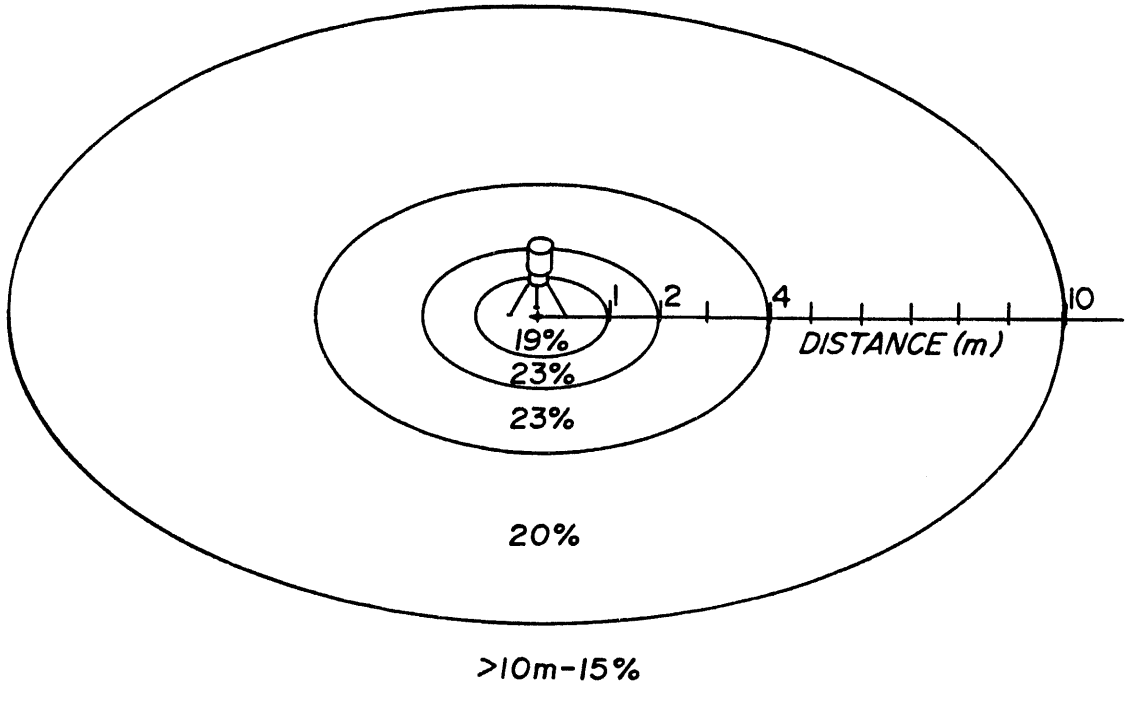


Figure I.1. Contribution to total 662 keV primary flux at 1 m above ground for a typical $^{137}Cs$ source distribution.

## ACKNOWLEDGMENTS

The authors acknowledge the work of past and present EML colleagues who have contributed so much over the years to the field of environmental radiation research and the application of *in situ* spectrometry. In particular we note the accomplishments of Wayne M. Lowder, Harold L. Beck and Carl V. Gogolak in the field. We also call attention to the adoption of the techniques described herein and the developments that have been made in the U.S. and around the world.

Some of the material presented here is taken from a draft that has been prepared for the International Commission on Radiation Units and Measurements (ICRU, in press). This material, together with additional contributions from other authors, is due to be published as a formal ICRU report on *in situ* gamma-ray spectrometry. In addition, many of the figures and tables appearing in this tutorial have been taken from other EML publications in the subject area.

# TABLE OF CONTENTS

# SECTION 1. INSTRUMENTATION

## DETECTORS

Although measurements can be conducted with sodium iodide (NaI) scintillation detectors, as they were in the 1960s, the energy resolution of Ge solid-state detectors and the fact that they are available with efficiencies as great as that of a 3x3 inch NaI detector make them the detectors of choice. As with any counting system, the size of the detector that is needed is related to the source strength, the counting time, and the desired statistical counting error. For typical environmental radiation fields, a detector with a quoted 25% efficiency would be large enough to give a 5% (1 $\sigma$) counting error for natural emitters given a 1 hour count time. A quick 10 minute count would be sufficient to provide lower limits of detection on the order of 100 Bq $m^{-2}$ for many common fission products residing at the surface of the soil. Higher sensitivity and/or reduced counting times can be achieved with larger detectors. Depending upon the application, a smaller detector might actually be a better choice in order to reduce counting dead time when making measurements in highly contaminated areas.

Another consideration is the choice between a P type and an N type Ge crystal. For applications that involve the measurement of low energy gamma rays, such as from $^{241}Am$ (59.5 keV), the N type has better sensitivity. Figure 1.1 shows a comparison in the efficiency between two typical detectors.

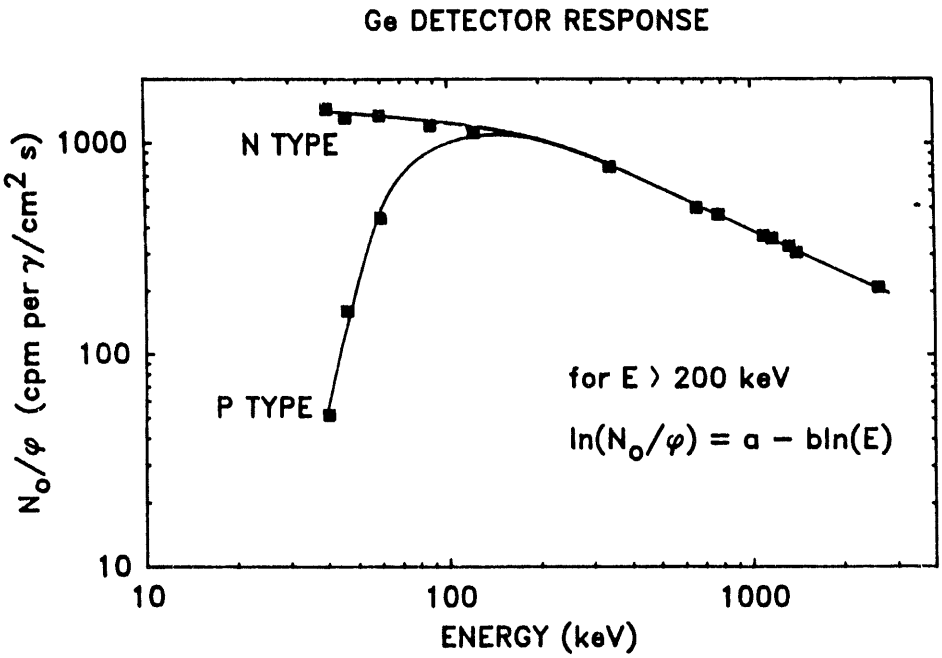


Figure 1.1. Comparison in the efficiency between two typical detectors.

Older lithium drifted Ge detectors can function perfectly well, however, the fact that intrinsic or high-purity Ge detectors can warm up without damage makes them the most suitable for field work.

Quality Ge detectors can be expected to have energy resolutions of 2 keV or better at 1332 keV. Better energy resolution allows a greater separation of two peaks that are close in energy. Also, each individual peak is narrower and therefore lower statistical counting errors are achieved since there is less continuum counts under the peak.

Modern Ge detectors are equipped with built-in preamplifiers. For field work where battery power is used, it is important to specify a low-power preamplifier when ordering a detector. This will extend the operational time in the field since the preamplifier is a principal draw on power.

Although measurements in the field can be performed with a Ge detector in almost any type cryostat-dewar configuration, performance and ease of handling is best achieved with a small dewar (1 to 2 liters) that can be tripod mounted with the detector facing down. For convenience, a 24 hour liquid nitrogen holding time is desirable as this then requires filling only once a day, although it may be safer to maintain a twice a day schedule. Ge detectors can also be cooled with electrically powered apparatus, however, this may not be as convenient for field use with battery-powered equipment. It is possible to mate small dewars to automatic filling apparatus in the laboratory or to larger gravity-feed storage dewars. As for orientation, a detector facing sideways (the axis of symmetry parallel to the ground) should be avoided because it introduces complicated angular corrections.

## PULSE HEIGHT ANALYZERS

A Ge detector can be connected to a full laboratory instrumentation package that is carried in a van and powered with a motor generator or battery bank. This was the norm in the early days of field spectrometry. Today, it is far more convenient to make use of portable battery-powered analyzers that are specifically designed for field work. These units not only serve as multichannel pulse height analyzers, but they also provide preamplifier power and high voltage to the detector. This type of analyzer with the Ge detector and a set of connecting cables is all that is needed for a complete spectrometry system. Also available now are portable laptop computer-based systems which have the capability to run more sophisticated analysis programs. An overnight recharge is generally sufficient to provide 8 hours of operational time in the field for either the full-function analyzer or the computer-based system. In the latter case, the computer can be shut off to conserve its own limited battery supply, while a spectrum continues to collect in the memory of the analyzer base unit.

One additional component needed for practical application of *in situ* spectrometry is a method of spectrum storage since it is likely that many spectra will be collected during the course of a site investigation. Some portable analyzers have built-in mini-cassette data storage capability, while others rely on an external portable audio cassette recorder. The PC-based systems have the advantage of being able to store numerous spectra directly on the internal disk drive.

## FIELD SETUP

The ideal site for collecting a spectrum would be a large (20 m diameter or more) flat, open area with little or no natural or man-made obstructions. The area to be measured can be scanned first with a suitably sensitive survey meter to insure that there is rough uniformity in background dose rate. It is also possible to move the Ge detector about and obtain quick spectra (1 to 5 minutes), observing that a full absorption peak count rate does not change substantially for a nuclide under study. For measuring fallout that was deposited in the past, the land should not have been disturbed by plowing or by wind or water erosion. For standard measurements, the detector (Ge crystal) should be at a height of 1 m above the ground, although a variation of as much as 50 cm in either direction will not introduce a large error. While collecting a spectrum, personnel should stand away from the detector. Since the operator may wish to examine the spectrum during collection, it is best to position the analyzer away from the detector using cable lengths of a few meters.

As with any gamma-ray spectrometer system, the amplifier gain and analyzer conversion rate must be adjusted to provide a spectrum in the energy region of interest. For environmental gamma radiation, this would be from about 50 keV out to 2.615 MeV, normally the highest energy line seen. For a 4000 channel analyzer, a conversion rate of 1 keV per channel will suffice in most cases, although 0.5 keV per channel may be desirable in certain situations to take advantage of the higher energy resolution of the detector at low energies.

# SECTION 2. THEORY

## BASIC CALIBRATION PARAMETERS

For sample analysis in the laboratory, calibrations are generally performed with solutions in the same counting geometry or spiked matrices such as soil and vegetation. In principle, one could calibrate a Ge detector for field use with very large (approaching an infinite half-space) calibrated areas as well. A far more convenient and flexible approach is to calculate the flux distribution on the detector for a given source geometry, determine the detector response with calibrated point sources and then perform an integration.

The fundamental quantities used for *in situ* spectrometry include full absorption peak count rate (N), fluence rate ($\phi$), and source activity (A). In practice, one would like a single factor to convert from the measured peak count rate in a spectrum to the source activity level in the soil or the dose rate in air. This factor can be calculated from three separately determined terms as follows:

$$\frac{N_f}{A} = \frac{N_f}{N_o} \cdot \frac{N_o}{\Phi} \cdot \frac{\Phi}{A} \tag{2.1}$$

where $N_f/A$ is the full absorption peak count rate at some energy, E, from a gamma transition for a particular isotope per unit activity of that isotope in the soil; $N_o/\phi$ is the full absorption peak count rate per unit fluence rate for a plane parallel beam of photons at energy, E, that is normal to the detector face; $N_f/N_o$ is the correction factor for the detector response at energy, E, to account for the fact that the fluence from an extended source in the environment will not be normal to the detector face but rather distributed across some range in angles; and $\phi/A$ is the fluence rate at energy, E, from photons arriving at the detector unscattered due to a gamma transition for a particular isotope per unit activity of that isotope in the soil.

The term $N_o/\phi$ is purely detector dependent, while the term $N_f/N_o$ is dependent on both the detector characteristics and the source geometry. These two terms will be covered in the following section on detector calibration. The term $\phi/A$ is not dependent on the detector characteristics but rather on the source distribution in the soil and will be dealt with in the following sections.

## UNSCATTERED FLUX

The theoretical model for an *in situ* measurement is illustrated in Figure 2.1. A gamma detector is located above a source that is distributed in, or deposited on, a volume of soil. Let $r_D$ be the vector which designates the position of the detector relative to the origin O. Moreover, let r designate the position of a differential volume of soil, and let $r_i$ designate the location of the air-ground interface. For a gamma source of energy E, the total unscattered flux is given by:

$$\Phi = \int_V \frac{f(r)}{4\pi(r_D - r)^2} \exp\left[ - \frac{\mu_s}{\rho} \rho(r_i - r) - \frac{\mu_a}{\rho_a} \rho_a(r_D - r_i) \right] dV \qquad (2.2)$$

where f(r) is the source strength at r, $\mu_s/\rho$ is the mass attenuation coefficient for soil ($cm^2\ g^{-1}$) and $\mu_a/\rho$ is the mass attenuation coefficient for air.

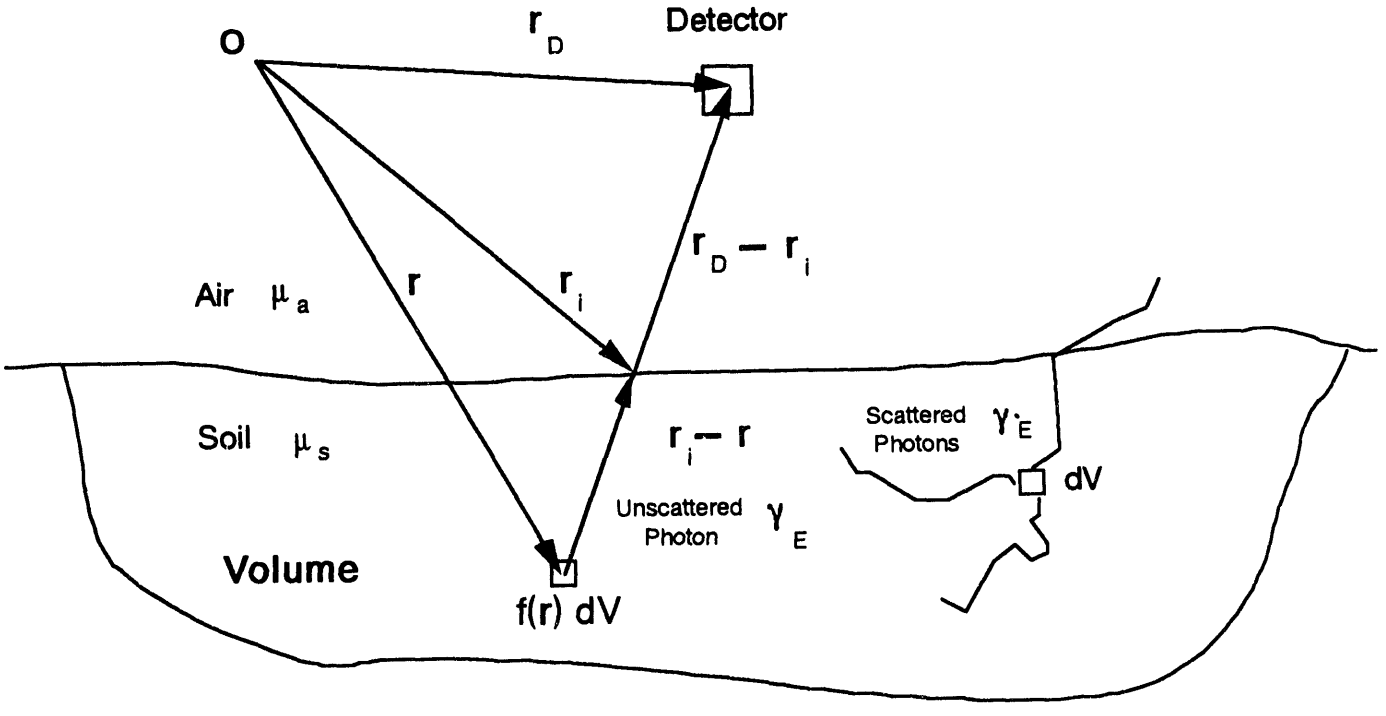


Figure 2.1. Theoretical model for an *in situ* measurement.

## SOURCE DISTRIBUTIONS

The most common natural sources of gamma radiation in the environment are the gamma emitters in the $^{238}U$ and $^{232}Th$ series and $^{40}K$. Anthropogenic sources include deposition from weapons testing and reactor effluent in the form of fallout. It is generally assumed that activities of fallout in the soil vary only with depth, while the natural radionuclides would be distributed uniformly.

The distribution of naturally occurring gamma emitters can then be expressed as

$$f(z) = S_V \qquad (2.3)$$

where $S_V$ is the soil activity per unit volume (photons/$cm^3$-s). In the case of fallout that has not been driven into the soil, such as fresh fallout from weapons testing, a plane source would seem most plausible. We have

$$f(z) = S_A \delta(z - z') \tag{2.4}$$

where $S_A$ is the surface activity (photons/cm$^2$-s) and z' is the distance from the detector to the air-ground interface. Aged fallout is reasonably approximated by an exponential distribution of the form

$$f(z) = S_o \exp\left(\frac{-\alpha}{\rho}\rho z\right) \tag{2.5}$$

where $\alpha$ is the inverse of the relaxation length (cm), $\rho$ is the soil density (g cm$^{-3}$), and $S_o$ is the surface activity (photon/cm$^2$-s).

In general, one relaxation length is that thickness of shield that will attenuate the flux to 1/e of its original density. Since we are dealing with a source term, the source depth parameter, $\alpha/\rho$, indicates the degree of self-absorption that will occur due to the penetration of the fallout into the soil matrix. For example, assuming a soil density of 1.6 g cm$^{-3}$ and a relaxation length of 1 mm will yield a source depth parameter of 6.25 cm$^2$ g$^{-1}$. The relaxation length in this case indicates that the fallout has penetrated the soil to the extent that 63% of the activity is contained within the first millimeter of soil. This is considered to be a very shallow distribution. Alternatively, a relaxation length of 10 cm will yield a source depth parameter of .0625 (cm$^2$ g$^{-1}$), and this is considered to be a deep distribution. We note that the product $\rho z$ is the mass depth and is more fundamentally related to flux than linear depth z because the number of atoms per unit length of soil is dependent upon the soil density. For the remainder of this section we will always assume a soil density of 1.6 g cm$^{-3}$.

It is convenient to think of the uniform and plane distributions as special cases of the exponential distribution. The plane distribution is obtained in the limit $\alpha \rightarrow \infty$, and the uniform distribution is the case where $\alpha = 0$. It must be pointed out that in terms of evaluating equation 2.2 for the flux, each case must be treated separately. The flux for a uniform distribution, for example, cannot be obtained in the limit $\alpha \rightarrow 0$. In the case of a uniform distribution, we are specifically referring to the natural emitters whose concentration is independent of depth, while in the case of fallout deposition, the flux from a uniform distribution obtained in the limit $\alpha \rightarrow 0$ must, as we shall see later, vanish.

In general any distribution that varies in the z direction can be approximated by a superposition of plane sources buried at various depths.

$$f(z) = \sum_i S_i \delta(z - z_i) \tag{2.6}$$

This distribution is useful for the case where there is markedly different soil strata of varying nuclide concentration.

The arrangement suggested in Figure 2.1 can be simplified by assuming a flat air-ground interface and infinite volume of soil. This particular geometry is referred to as an infinite

half-space. Our specific model used to evaluate this case is illustrated in Figure 2.2. The detector is positioned at the origin, with the air-ground interface located a distance h below the detector. Hence, the ideal set-up for an *in situ* measurement would be a large, flat open field with little or no surface features and no obstructions that could substantially reduce the photon flux.

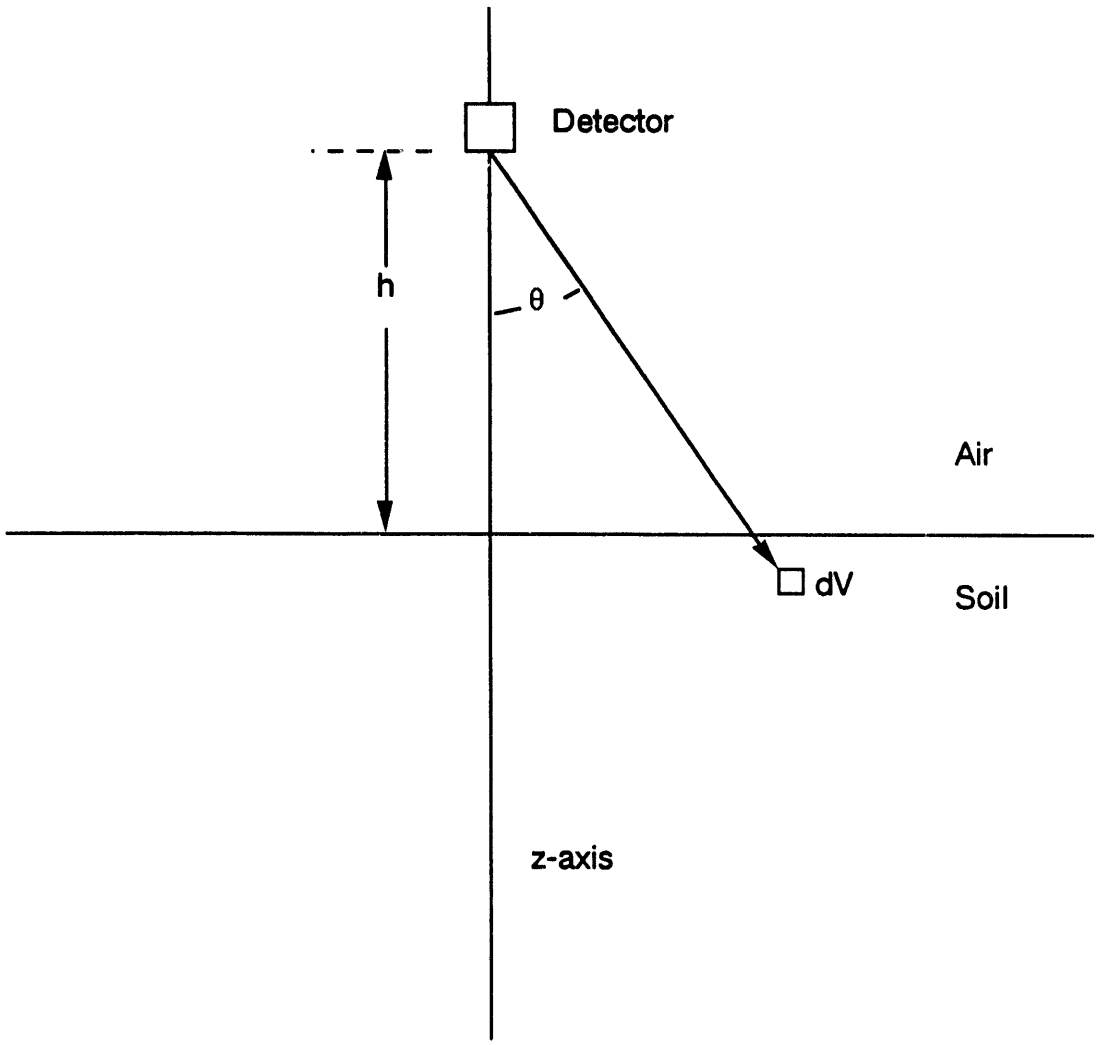


Figure 2.2. Theoretical model used in calculating flux.

## PHOTON FLUX CALCULATION

Assuming an exponential distribution, equation 2.2 can now be written as

$$\Phi = 2\pi \int_h^\infty \int_1^\infty \frac{S_o}{4\pi\omega} \exp\left(-\frac{\alpha}{\rho}\rho z\right) \exp\left[-\frac{\mu_s}{\rho}\rho(z-h)\omega - \frac{\mu_a}{\rho_a}\rho_a h\omega\right] d\omega dz \qquad (2.7)$$

where $\omega = \sec\theta$, $\rho(z - h)$ is the mass depth of soil, and $\rho_a h$ is the mass depth of air. The exact solution to (2.7) is

$$\frac{\Phi}{S_o} = \frac{1}{2}\left[E_1\left(\frac{\mu_a}{\rho_a}\rho_a h\right) - \exp\left(\frac{\alpha}{\rho}\frac{\rho}{\mu_s}\frac{\mu_a}{\rho_a}\rho_a h\right) E_1\left[\left(1 + \frac{\alpha}{\rho}\frac{\rho}{\mu_s}\right)\frac{\mu_a}{\rho_a}\rho_a h\right]\right] \qquad (2.8)$$

The function $E_1(x)$ is known as the exponential integral and is defined as

$$E_1(x) \equiv \int_x^\infty \frac{e^{-t}}{t}\, dt \qquad (2.9)$$

Figure 2.3 is a plot of $E_1(x)$. It is important to note how rapidly $E_1(x)$ falls off with x.

For a uniform distribution we have

$$\Phi = 2\pi \int_h^\infty \int_1^\infty \frac{S_V}{4\pi\omega} \exp\left(-\frac{\mu_s}{\rho}\rho(z-h)\omega - \frac{\mu_a}{\rho_a}\rho_a h\omega\right) d\omega dz \qquad (2.10)$$

where $S_V$ is the soil activity per unit volume (photons $cm^{-3}$-s). The exact solution to (2.10) is

$$\frac{\Phi}{S_V/\rho} = \frac{1}{2}\frac{\mu_a}{\rho_a}\frac{\rho}{\mu_s}\rho h\left(\frac{\exp[(\mu_a/\rho_a)\rho_a h]}{(\mu_a/\rho_a)\rho_a h} - E_1\left(\frac{\mu_a}{\rho_a}\rho_a h\right)\right) \qquad (2.11)$$

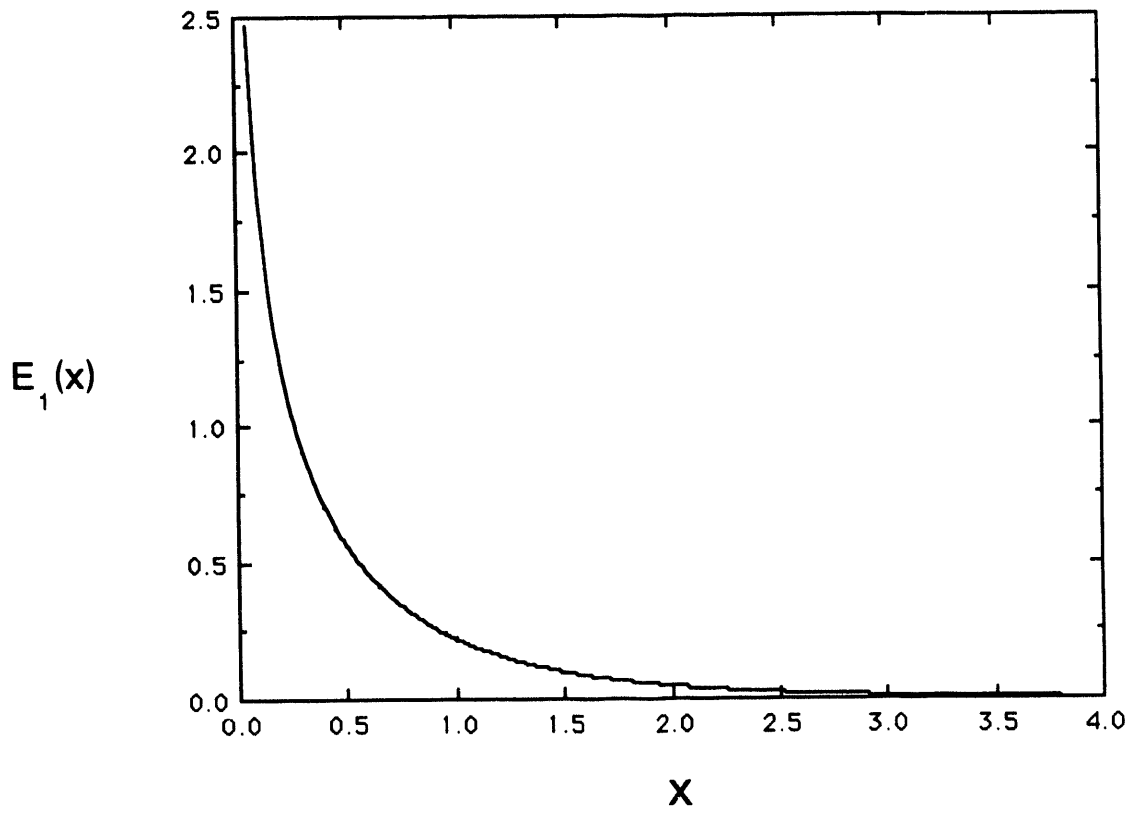


Figure 2.3. Exponential Integral $E_1(x)$.

The flux from a plane source distribution can be obtained from equation 2.8 in the limit $\alpha/\rho \rightarrow \infty$.

For a plane source distribution we have

$$\frac{\Phi}{S_o} = \frac{1}{2} E_1\left(\frac{\mu_a}{\rho_a} \rho_a h\right) \tag{2.12}$$

Flux computations can be performed on a case by case basis, however, it is convenient and sufficiently accurate to use the results of Beck et al. (1972), which were performed for a standard height of 1 m for a soil with a representative mix of elements. The total fluence is tabulated in Table 1 of that report for various values of $\alpha/\rho$ at different energies. The distribution with respect to the angle $\theta$ can be found in Table 6 of the same report.

## DEPENDENCE OF THE FLUX ON THE PARAMETERS $\alpha/\rho$ AND $\mu_s/\rho$

We see in equation 2.8 that the flux from an exponentially distributed source depends on the product $(\alpha/\rho)/(\rho/\mu_s)$. This term can be expressed as $(1/\mu_s)/(1/\alpha)$, which is just the mean-free-path (MFP) for a photon of energy E in soil per unit relaxation length. If $(1/\mu_s)/(1/\alpha) \geq 1$, then a minimum of 63% of the fallout is within 1 MFP of the air-ground interface. So for the case of a very shallow distribution, $(1/\mu_s)/(1/\alpha)$ can be quite large. Since the term $E_1[\mu_a/\rho_a\ (1 + (\alpha/\rho)/(\rho/\mu_s)(\rho_a h))]$ goes to zero faster than the exponential diverges, the flux from a shallow distribution approaches the flux from a plane source distribution in the limit $\alpha/\rho \rightarrow \infty$. This fact is reflected in Figure 2.4. Here we have a plot of $\phi/S_o$ as a function of $\alpha/\rho$ for several different energies. Note the flatness of the graphs for $\alpha/\rho > 100$. However, since typical values for $\alpha/\rho$ obtained from soil samples rarely exceed 6.25 $cm^2\ g^{-1}$, and since the source geometry for this model assumes a perfectly smooth interface, the case of a plane source distribution is unrealistic for most *in situ* measurements.

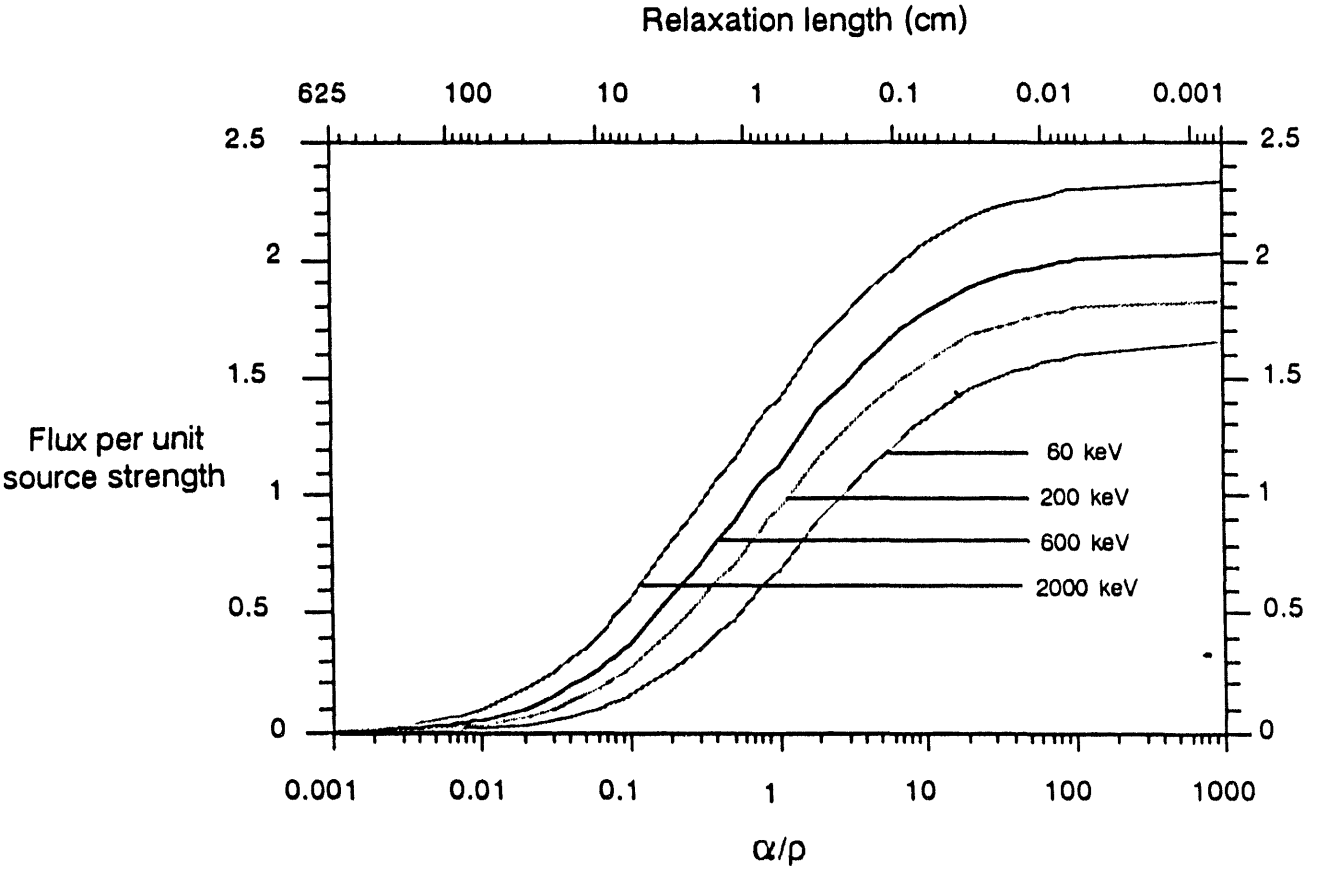


Figure 2.4. Flux per unit source strength for an exponential source distribution as the function of the source depth parameter $(\alpha/\rho)$ and the relaxation length $(1/\alpha)$ for four different energies.

For the case of a very deeply distributed source, $(1/\mu_s)/(1/\alpha)$ is nearly zero. It follows from equation 2.8 that in the limit $\alpha/\rho \rightarrow 0$, the flux vanishes. That is, the flux from a deeply distributed source has diluted its concentration to the point that no photons are able to reach the detector without interacting with the soil. This too is reflected in Figure 2.4. Note that the flux approaches zero as $\alpha/\rho \rightarrow 0$.

Figure 2.5 is a plot of the flux a function of energy for a uniform depth profile. It must be emphasized that this situation is not to be confused with the deeply distributed source described previously. The uniform source distribution arises primarily with the natural emitters and not from fallout.

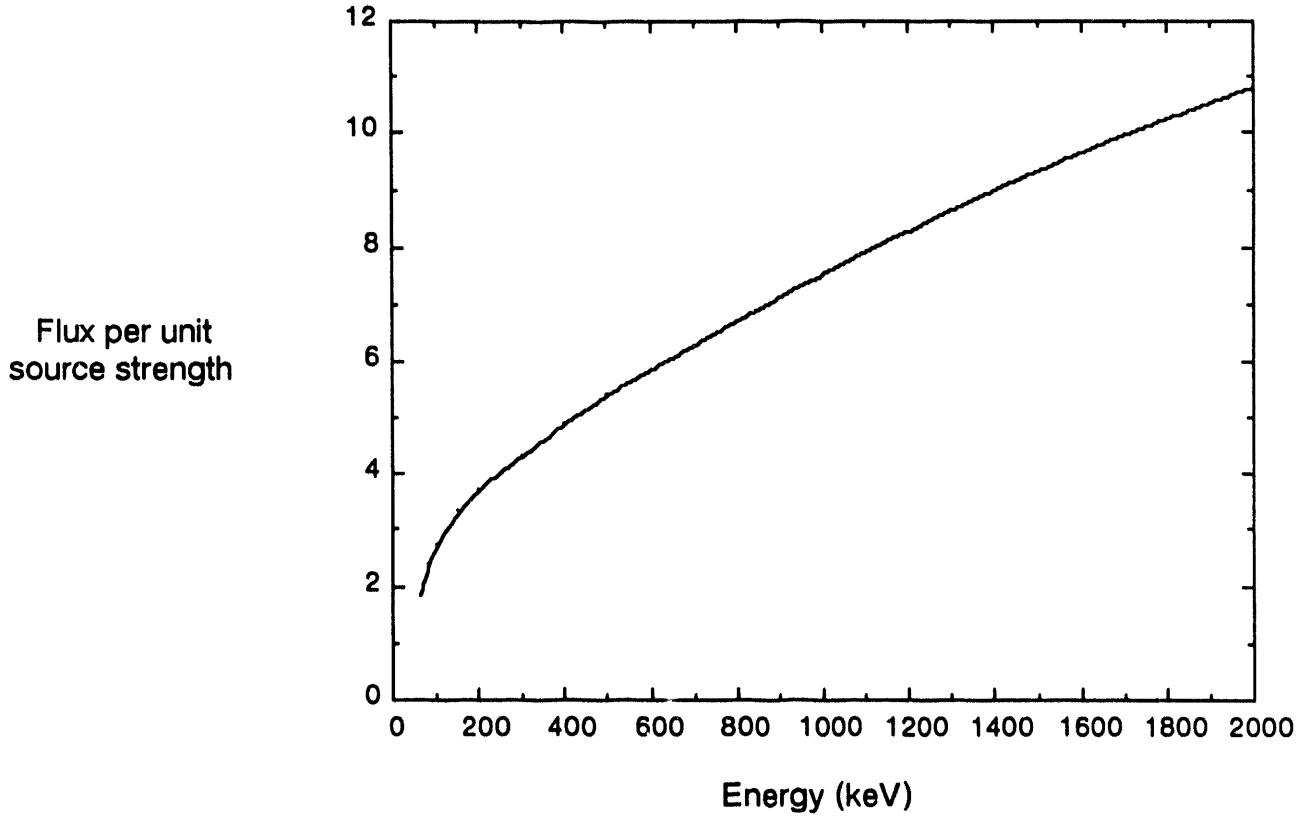


Figure 2.5. Flux per unit source strength for a uniform depth profile as a function of energy.

## DEPENDENCE OF THE FLUX ON THE SOURCE GEOMETRY

Figures 2.6 and 2.7 show the fraction of the total flux as a function of the horizontal distance from the detector for several energies. Figure 2.6 is for a deep distribution, while Figure 2.7 is for a shallow one. The essential point is the relationship between the source distribution and the contribution to the total flux from various horizontal distances. For $\alpha/\rho = 6.25\ cm^2\ g^{-1}$, roughly 40% to 50% of the flux comes from horizontal distances greater than 10 m, while for $\alpha/\rho = 0.0625\ cm^2\ g^{-1}$, only about 10% to 20% of the flux comes from distances greater than 10 m. The immediate implication of this fact is that for the accurate measurement of recent fallout deposition, corrections for a limited half space may be necessary if the site to be measured has obstructions within a 100-m radius.

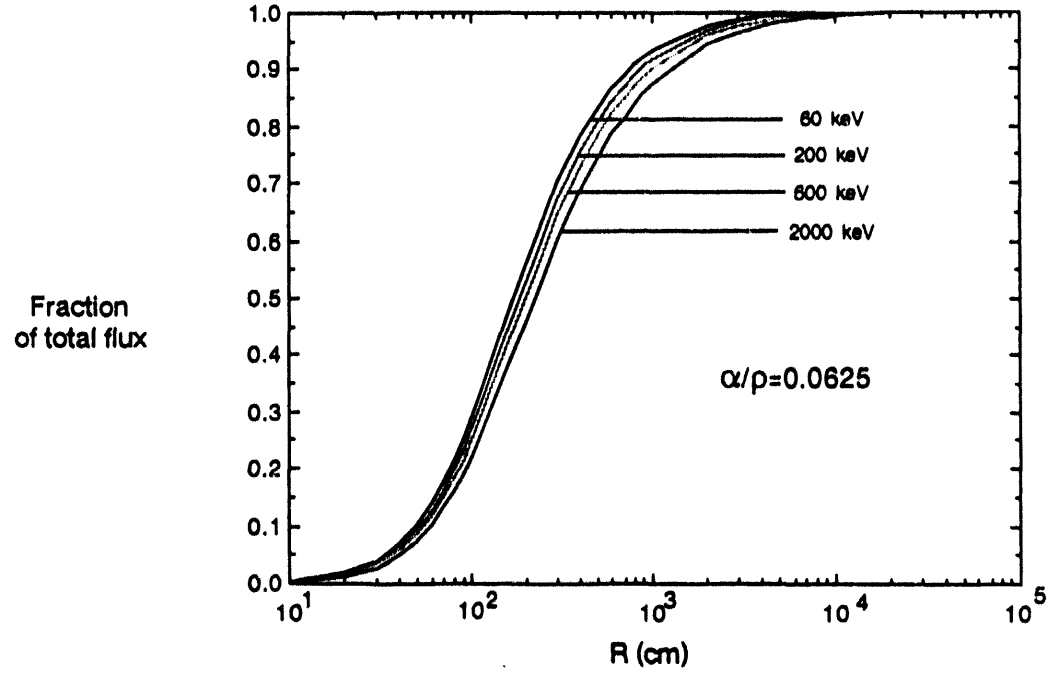


Figure 2.6. Fraction of the total flux as a function of radial distance from the detector for a source depth parameter $\alpha/\rho = 0.0625$.

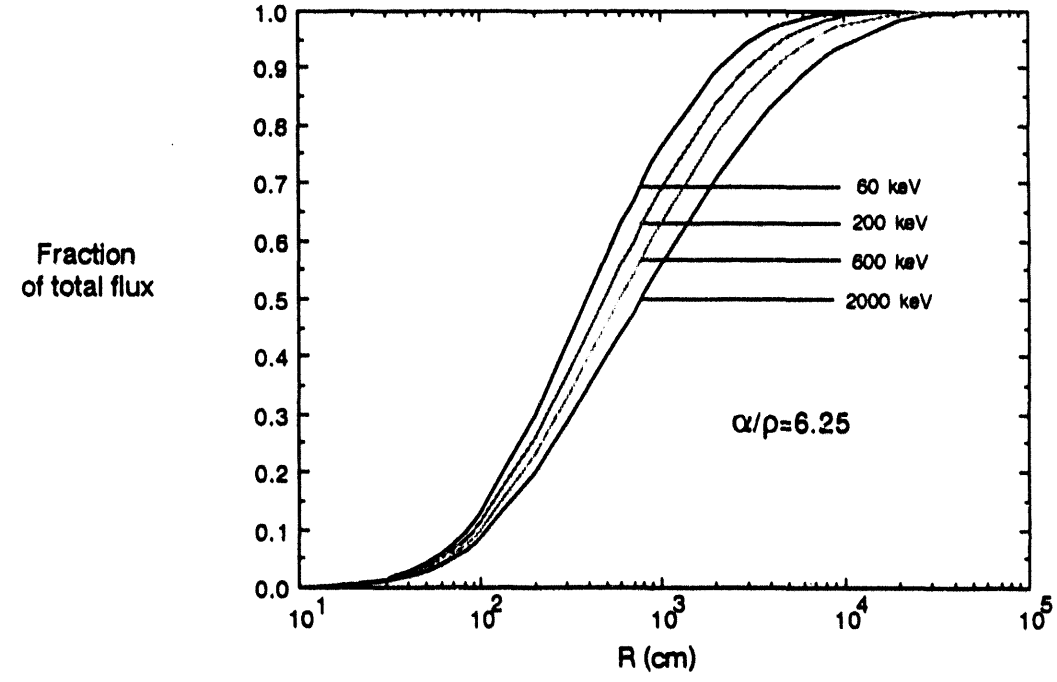


Figure 2.7. Fraction of the total flux as a function of radial distance from the detector for a source depth parameter $\alpha/\rho = 6.25$.

Figures 2.8 and 2.9 show the fraction of the total flux as a function of the linear depth beneath the air-ground surface interface for several energies. Figure 2.8 is for a deep distribution, while Figure 2.9 is for a shallow one. Here, the essential point is that even for a relatively deep distribution ($\alpha/\rho$ = 0.0625 $cm^2$ $g^{-1}$), over 90% of the total flux comes from the first 10 cm of soil. The situation is even more extreme in the case of a shallow distribution. In Figure 2.9 we can see that roughly 75% of the total flux comes from the first 1 mm of soil. In the case of $\alpha/\rho$ = 6.25 $cm^2$ $g^{-1}$, 63% of the total concentration lies within the first millimeter of soil.

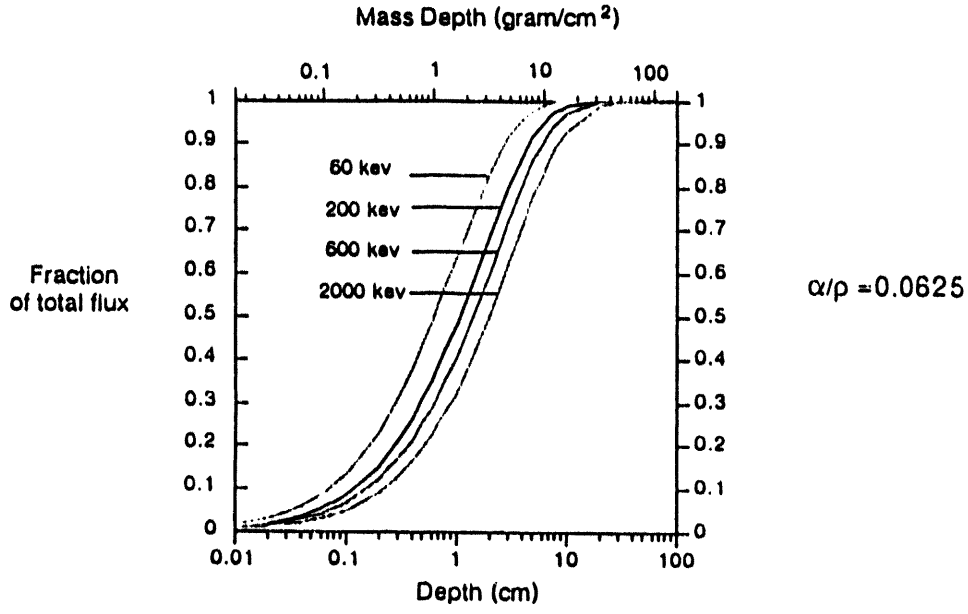


Figure 2.8. Fraction of the total flux as a function of depth and mass depth in the soil for a source depth parameter $\alpha/\rho$ = 0.0625.

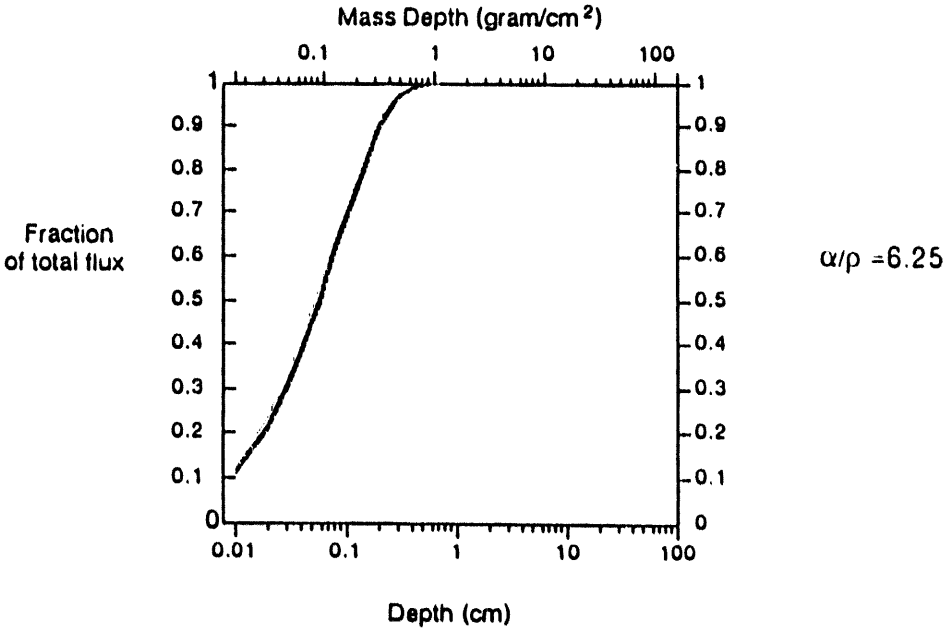


Figure 2.9. Fraction of the total flux as a function of depth and mass depth in the soil for a source depth parameter $\alpha/\rho$ = 6.25.

## OTHER FACTORS AFFECTING FLUX

Excessive ground roughness effectively provides additional self-absorption and therefore makes the source appear more deeply distributed.

Variations in soil density are effectively factored out of the relationship because the concentration of radionuclides in the soil is given per unit mass. Thus, a soil with twice the normal density will have half the concentration and therefore provide half the flux.

The precise soil composition is generally not needed. A typical soil composition might consist of 63% silicon dioxide, 14% aluminum oxide, 5% iron oxide, 5% carbon dioxide, and 10% water. Varying the soil composition will affect the flux through the mass attenuation coefficients. The variation in soil composition will, in the very extreme cases, result in a few percent error in the flux for medium and high energy photons. Figure 2.10 shows the relative error in the flux for a 1% deviation from the assumed mass attenuation coefficient of soil as a function of the source depth parameter. As one would expect, the more deeply distributed source is more sensitive to the specific soil composition. Clearly, a low energy, deeply distributed source requires the specific mass attenuation coefficient to ultimately determine an accurate source activity.

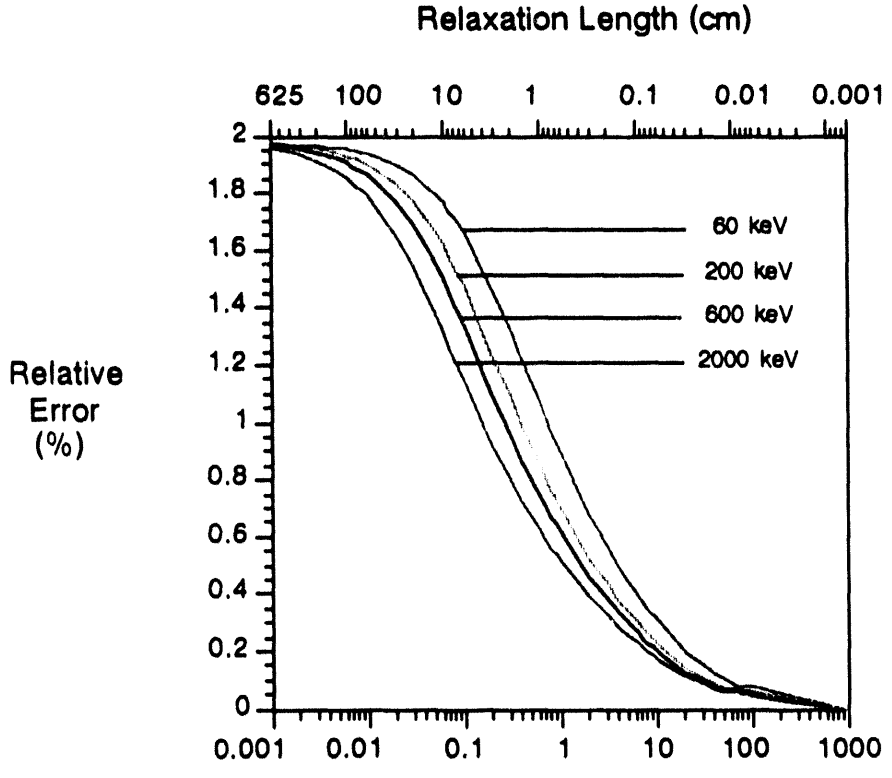


Figure 2.10. Relative error in the flux due to a 1% uncertainty in the mass attenuation coefficient of soil.

Since at a height of 1 m, the mass depth of air is typically one-tenth the mass depth of soil, uncertainty in the flux due to a deviation from the assumed mass attenuation coefficient of air is regarded as negligible. However, variations in the density of air could produce as much as a 5% to 7% error in the flux for a very shallow distribution. For purposes of *in situ* spectrometry, variations in the air density occur only with altitude. Figure 2.11 shows the relative error in the flux as a function of height for several different energies and two different source distributions. We have assumed that the density of air decreases exponentially with the height above sea level and a scaling height of 7 km. This figure demonstrates the necessity to correct for air density for fresh fallout at high altitudes.

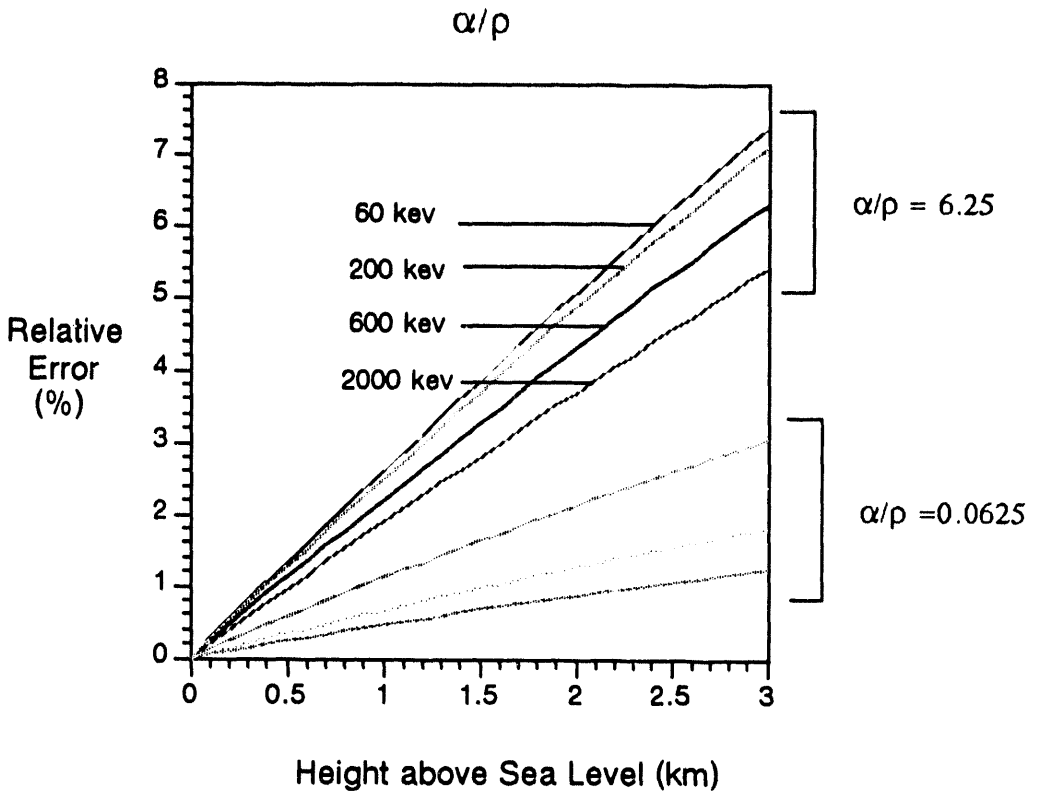


Figure 2.11. Relative error in the flux due to changes in the air density as a function of height above sea level. For the $\alpha/\rho = 0.0625$, the order of the energies is identical to 6.25.

# SECTION 3. DETECTOR CALIBRATION

## RESPONSE AT NORMAL INCIDENCE

The response of the detector to photons at normal incidence is represented by the term $N_o/\phi$ which was introduced in equation 2.1 in the previous section. In general, the response of a detector to incident photon fluence is a complex function of a number of factors such as crystal size, shape, mounting, housing, and inactive volume regions. Estimates of these parameters can be provided by the manufacturer and then used as input to computer codes for determining the detector efficiency as a function of energy. More commonly, experimental determinations of detector response are performed using certified calibration sources. One standard measure of a Ge detector performance is the efficiency at 1332 keV relative to a 3x3 inch NaI crystal. This measurement is performed with a $^{60}$Co point source positioned 25 cm from the detector face at normal incidence. For purposes of *in situ* gamma-ray spectrometry, a more meaningful measurement is to determine the full absorption peak count rate per unit incident fluence rate at a given energy for plane parallel radiation which requires a larger source to detector distance. In the case of long Ge crystals, the standard measurement distance of 25 cm underestimates the efficiency that would be achieved for *in situ* spectrometry since the distance to the effective crystal center is larger. True plane parallel incidence would be accomplished for a point source at infinite distance. For practical applications, however, a source distance of 1 to 2 m can suffice considering that the dimensions of a Ge crystal are on the order of a few cm or less.

The full absorption peak count rate N, sometimes referred to as the peak area, is computed as the sum of the counts across those channels that represent a peak in the spectrum minus the counts in the underlying continuum, sometimes referred to as the baseline or background. All modern full-function analyzers and software analysis packages allow the user to set up a region of interest (representing the peak) and the peak area is automatically calculated. Generally, three to five channels on both the low and high energy side of the peak are used as a basis to infer the continuum counts.

The fluence rate, $\phi(E)$, at the detector is given by the expression

$$\Phi(E) = \frac{R(E)}{4\pi x^2} \tag{3.1}$$

where R(E) is the gamma-ray emission rate at that energy and x is the source to detector distance. The attenuation effect of the source encapsulation should be taken into account along with that of the air between the source and detector, particularly for low energy gamma rays and large values of r.

The determination of the ratio of $N_o$ to $\phi(E)$ must be done at several different energies over the effective operating energy range of the instrument. For environmental gamma radiation this range would be up to 2.615 MeV, a principal gamma-ray line of $^{208}$Tl in the naturally occurring $^{232}$Th series (although there may be applications for studying N-16 near operating reactors. in which case an energy range of up to 7 MeV). The effective low end

point will depend upon the type of detector, which would be about 60 keV for P-type Ge and down to 10 keV for N-type.

Although almost any certified gamma source can be used to measure the detector efficiency at a particular energy, the use of longer-lived isotopes is recommended so that measurements can be repeated throughout the lifetime of the same detector. In addition, the use of the same set of sources for two different detectors will reduce systematic differences in their responses. It is also effective to use multiple gamma emitters such as $^{152}$Eu and $^{154}$Eu since they can provide many data points across a wide energy range. While these isotopes generally introduce some difficulty in the interpretation of the detector response for close-in geometries due to the effects of cascade coincidence summing, the effect is negligible at source distances of a meter or more. Also, $^{241}$Am (59.5 keV), $^{137}$Cs (661.6 keV), and $^{60}$Co (1173.2 keV and 1332.5 keV) are common isotopes that can provide data points at low, medium, and high energies, respectively. Although it has a relatively short half-life of 1.9 years, $^{228}$Th provides a crucial high energy point at 2.615 from its progeny, $^{208}$Tl. Mixed gamma-ray point sources specifically made for calibrating Ge detectors are regularly available from the National Institute of Standards and Technology (NIST).

A precise determination of $N_o/\phi(E)$ should take into account that the calculation of the fluence rate at the detector will depend upon the distance from the point source to average point of interaction within the crystal and the window to crystal distance. At low energies (<~100 keV), the penetration of the photons into the crystal is minimal and the distance to the front surface can be taken to be the value of r plus the manufacturer's estimated window to crystal distance. For high energies (>~1 MeV), the value of r can be measured to the geometric midpoint of the crystal since the penetration is high and the interactions are spread throughout. For medium energies, the mean penetration into the crystal can be estimated from the photon cross section data for Ge or can be experimentally determined by plotting the inverse of the square root of the peak count rate versus the source to window distance for two or more distances. The intercept on the plots for a specific energy then represents the effective penetration into the crystal at that energy plus the window to crystal distance. An example of the results of this experimental determination are shown in Figure 3.1.

The precise value of r becomes less important as the source to detector distance increases relative to the crystal dimensions. For a crystal that is 6 cm long, the difference in the fluence rate at 1 m is close to 6% for front surface as opposed to crystal midpoint distances. At 2 m the difference is reduced to 3%.

Once the value of $N_o/\phi(E)$ has been determined at several different energies, a polynomial fit can be applied across the energy range. Alternatively, a simple straight-line fit on a log-log plot is adequate between 300 and 2000 keV. This simplest of approaches fits the data to within 3%. Since each source has some uncertainty in the quoted activity, a best fit straight line is perhaps a more realistic choice over a forced fit curve with many points of inflection. If suitable calibration sources are not available outside this energy range, extrapolations of the straight-line fit down to 200 keV and up to 3 MeV would generally not introduce significantly larger errors. For comparison, Figure 3.2 shows examples of calibration fits for eight different detectors of various sizes, as measured by the manufacturer's quoted relative efficiency at 1332 keV.

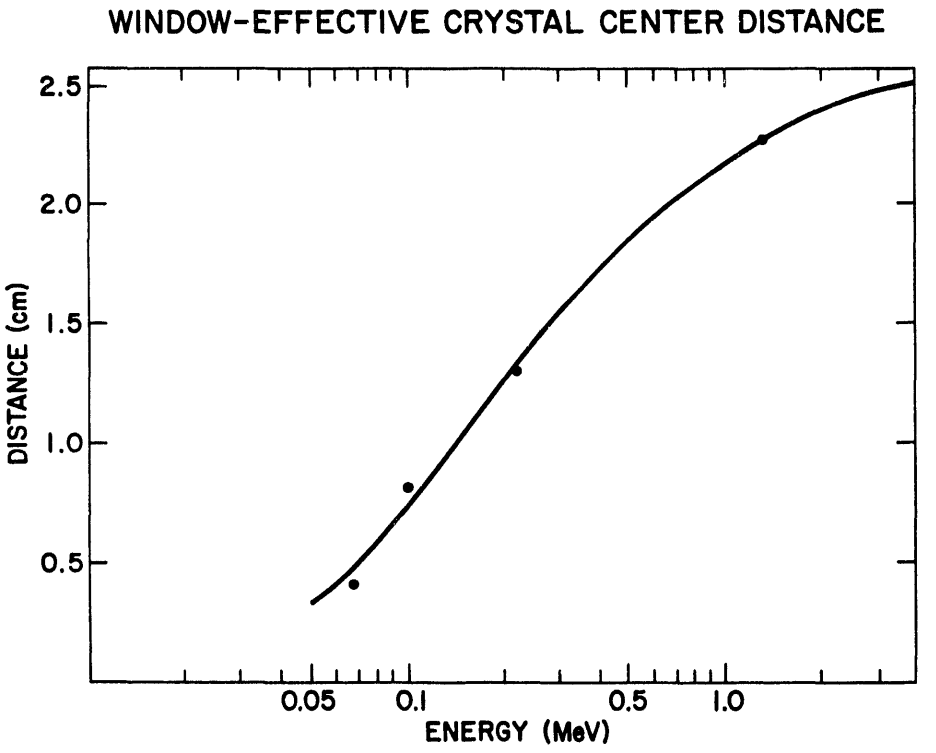


Figure 3.1. Window-effective crystal center distance as function of energy.

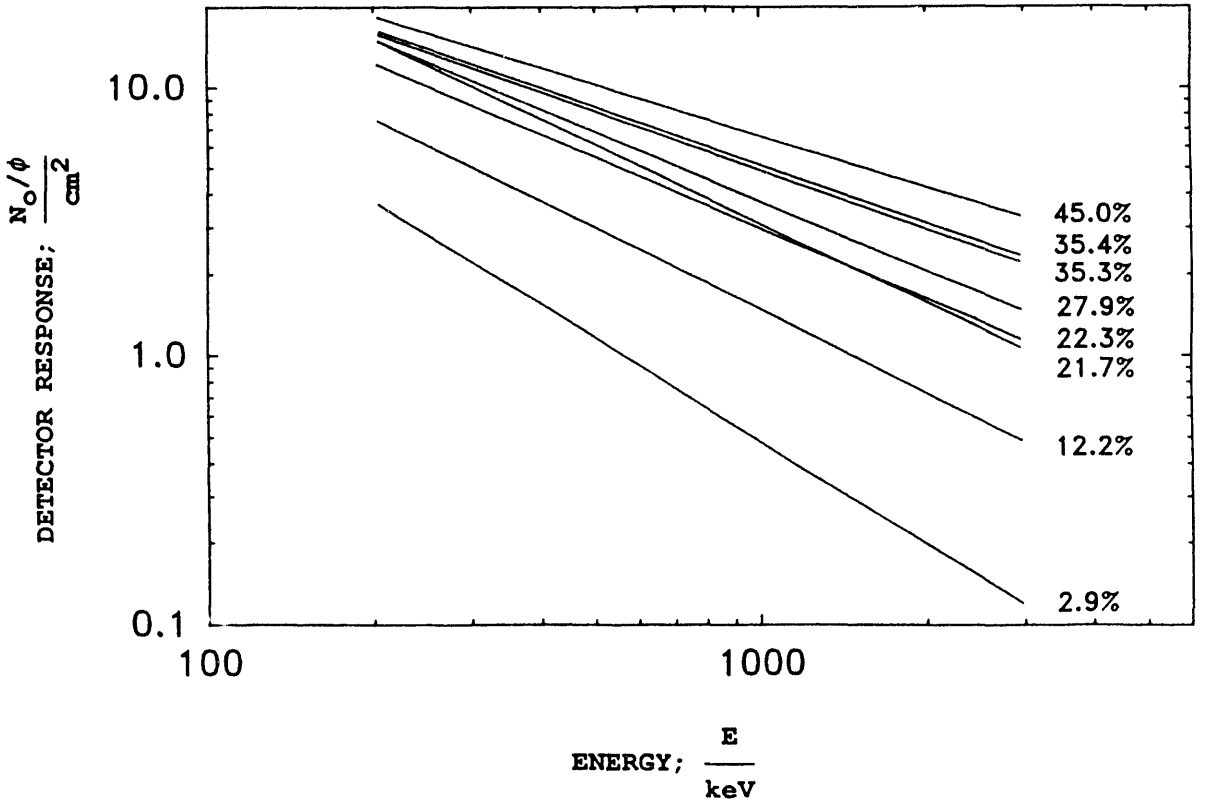


Figure 3.2. Detector response over the energy range 0.2 to 3.0 MeV for eight different detector efficiencies.

********

## *EXAMPLE 1*

*A Measurement of $N_o/\phi$ at One Energy*

*A $^{137}Cs$ source with an activity of 10.28 μCi as of January 1, 1980 is used. The energy is 662 keV, the gamma intensity is 85.2% and the half-life is 30.2 years. The measurement was performed in April 1991. The aluminum encapsulation is listed as attenuating the 662 photons by 1.2%. The mass attenuation coefficient for air at 662 keV is 0.076 $cm^2 g^{-1}$ and the air density is 0.0012 g $cm^{-3}$. The estimated effective crystal center is 1.2 cm from the detector face. The source is placed at a distance of 138.1 cm to the detector face. The measured peak count rate is 250.6 counts $min^{-1}$.*

1. *Calculate the gamma emission rate of the source.*

   *units conversion: 10.28 μCi x 37000 Bq $\mu Ci^{-1}$ = 380360 Bq*
   *half-life correction: 380360 Bq x exp(-0.693 x 11.3/30.2) = 293482 Bq*
   *gamma emission: 293482 Bq x 0.852 γ per disintegration = 250047 γ $s^{-1}$*

2. *Calculate the flux at the detector.*

   *source self-attenuation: 250047 γ $s^{-1}$ x .988 = 247046 γ $s^{-1}$*
   *air attenuation: 247046 γ $s^{-1}$ x exp(-138.1 x 0.076 x 0.0012) = 243954 γ $s^{-1}$*
   *geometry factor: 243954 γ $s^{-1}$ + [4π(138.1 cm + 1.2 cm)$^2$] = 1.001 γ $cm^{-2}$ $s^{-1}$*

3. *Calculate the ratio.*

   *$N_o/\phi$ = 250.6 cpm + 1.001 γ $cm^{-2}$ $s^{-1}$ = 250.3 counts $min^{-1}$ per γ $cm^{-2}$ $s^{-1}$*

********

********

## *EXAMPLE 2*

*Generation of an Efficiency Curve*

*Using the procedure shown in Example 1, the following data were generated with various point sources:*

| *Energy (keV)* | *$N_o/\phi$ (cpm per $\gamma/cm^2$ s)* |
|---|---|
| *60* | *490* |
| *122* | *1077* |
| *344* | *501* |
| *662* | *245* |
| *779* | *210* |
| *1086* | *155* |
| *1112* | *153* |
| *1408* | *128* |

*These data are plotted on log-log paper as shown below:*

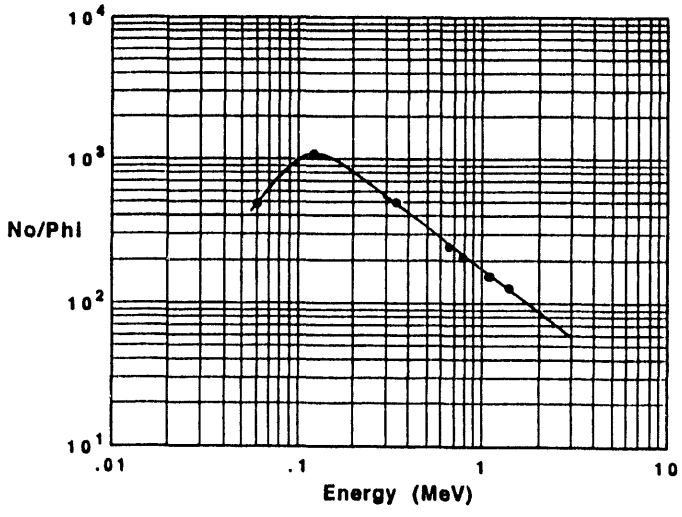


*Taking the data points at 0.3 MeV and 3 MeV off the straight-line portion of this fit, the slope of the line is*

$$\Delta y/\Delta x = [ln(550) - ln(60)] / [ln(0.3 - ln(3)] = 2.216/(-2.302) = -0.963$$

*The intercept occurs at $1n(E) = 0$, which is E = 1 MeV. This is seen to be 173 and $ln(173) = 5.15$. Thus the complete equation can be written as*

$$1n(N_o/\phi) = 5.15 - 0.963\ 1n(E)$$

*or*

$$(N_o/\phi) = e^{(5.15 - 0.963\ \ 1nE)}$$

*where E is in units of MeV. This equation can be used to compute the value of $N_o/\phi$ for any energy between 300 keV and 2 MeV.*

********

## ANGULAR RESPONSE

Although the response of a detector to photon flux at normal incidence provides a general measure of the sensitivity for *in situ* measurements, the actual full calibration of the detector for most applications involves the response at other angles of incidence because one is generally measuring extended sources in the environment and not aiming the detector towards a point source. In these circumstances, photons will be incident on the detector through the side wall and even possibly at angles corresponding to a photon path through the dewar. For this reason, some consideration must be given to the crystal shape, dewar size and detector orientation in the field.

Due to the cylindrical shape of the Ge crystal, it can be assumed that there is a uniform response about its axis of rotation. This can be checked experimentally for a detector to insure that the mounting structure has not introduced any substantial asymmetrical response characteristics. For typical applications in the field, the orientation of the detector should be with the axis of rotation perpendicular to the ground, thus eliminating any dependence on angle of photon incidence about the azimuth.

The response in the plane perpendicular to the detector face is generally not uniform. For the measurement of a source in a half-space geometry where the detector is faced toward the ground, the range of angles would be 0° (normal incidence to the detector face) to 90° (sidewall incidence). This would be the ideal orientation for measuring ground sources, i.e., facing down with the dewar overhead. Although it may seem unconventional, it is still possible to perform measurements over soil with the detector facing up and the dewar underneath. In this case, the range in the photon angles of incidence would be 90° to 180°, relative to the detector face. In either case, the detector response about the angles of photon incidence must be determined. This is accomplished by counting point sources at a fixed distance at least 1 m at several angles. The peak count rates at a given energy can be normalized to 0° incidence and fitted to a smooth curve on a plot. Figures 3.3 and 3.4 show examples for two different detectors across the full range in angles, 0° to 180°, where 0° represents normal incidence on the detector face. The data in Figure 3.3 are for a detector with a small 1.2-L cryostat, while the data in Figure 3.4 are for a detector with a dipstick cryostat in a 17-L dewar. In practice, this later detector would be situated facing up in the field and the flux would be incident in the range of 90° to 180°.

Whereas the total volume of the Ge crystal is closely related to the quoted efficiency, the shape of the crystal is the fundamental controlling factor for the variation in response at other than normal incidence. Based on theoretical considerations, and as found in experimental studies on detectors (Helfer and Miller, 1988), a cylindrical crystal with a length (L) greater than the diameter (D) will tend to have a higher response at angles off normal incidence. The response for a detector where L is less than D would tend to be opposite to this since less the surface area is presented to the fluence at sidewall incidence. The variation in response would be least for crystals where L ≈ D. In general, response variations with angle would be most pronounced at lower energies where the efficiency would be related to the effective area that intercepts the photon fluence. At higher energies, the angular response characteristics are less sensitive to the crystal shape since primary and secondary absorption occurs throughout the volume of the Ge crystal. To illustrate these characteristics, the responses (relative to normal incidence) for three different crystal shapes (as measured by the

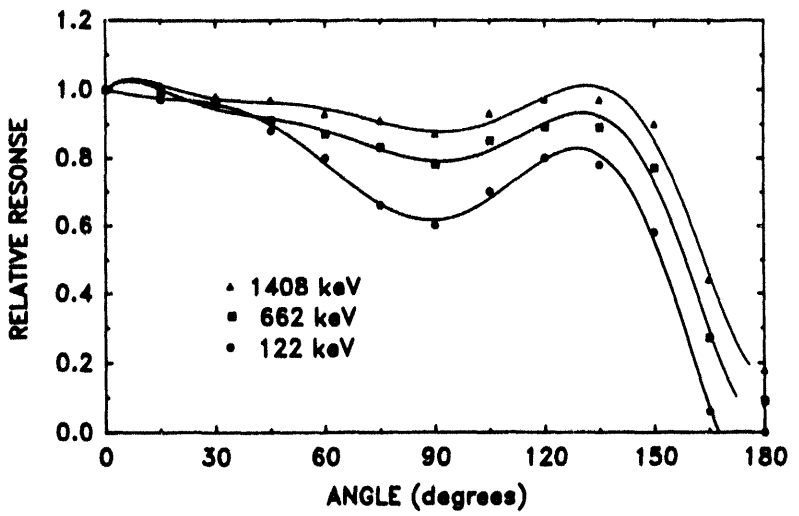


Figure 3.3. Angular response of a 21.7% efficiency detector with a length to diameter ratio of .59, for three energies.

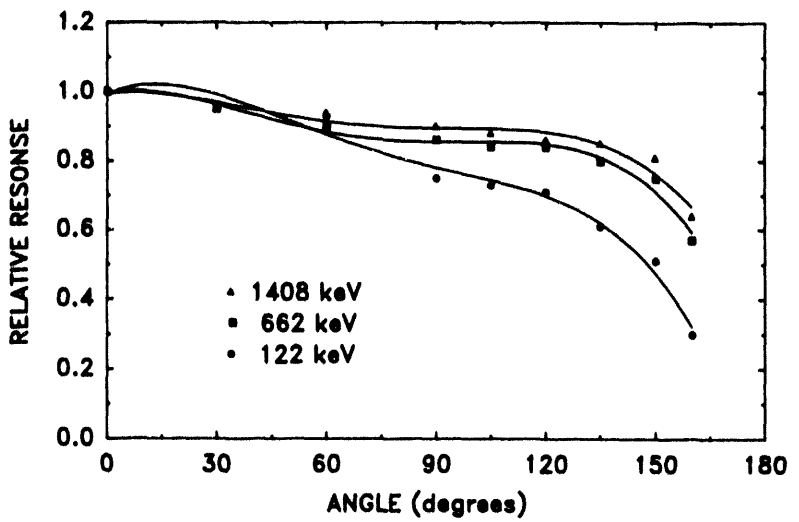


Figure 3.4. Angular response of a 27.9% efficiency detector with a length to diameter ratio of .80, for three energies.

L/D ratio) are presented for three separate energies in Figures 3.5, 3.6, and 3.7. These data are indicative of the general behavior that would be found for Ge detectors, although the exact angular response would be expected to vary among detectors with the same L/D ratio because of different sizes and variations in attenuation properties associated with mounting and housing. At very low energies (< 100 keV), the effects of attenuation by the detector mounting and housing material can substantially reduce the efficiency for flux incident on the detector sidewall and no general behavior can be predicted.

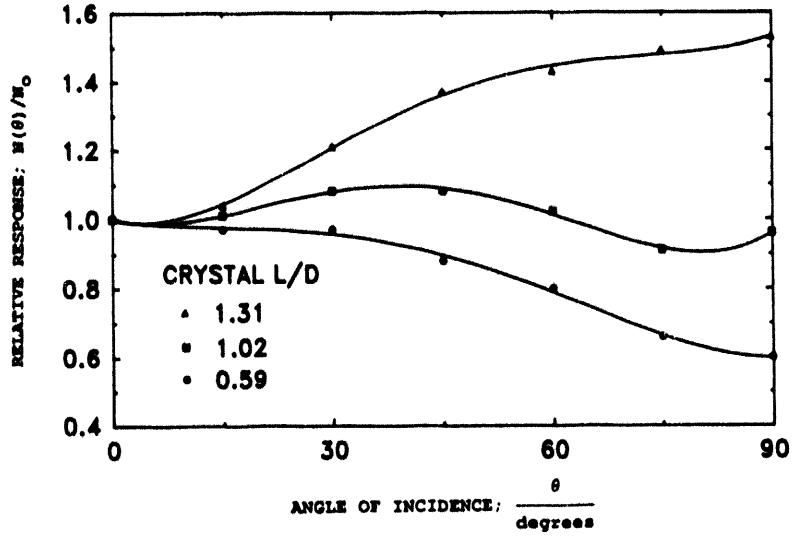


Figure 3.5. Angular response over the range 0-90° at 122 keV for three length-to-diameter ratios.

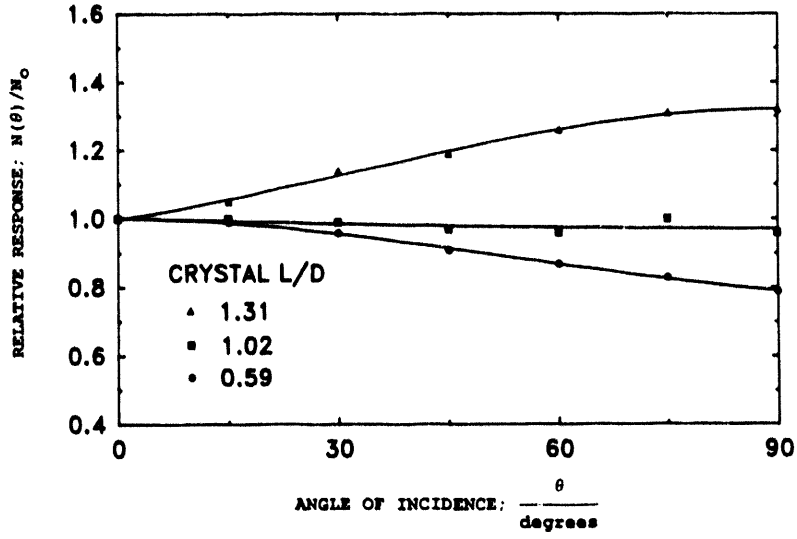


Figure 3.6. Angular response over the range 0-90° at 662 keV for three length-to-diameter ratios.

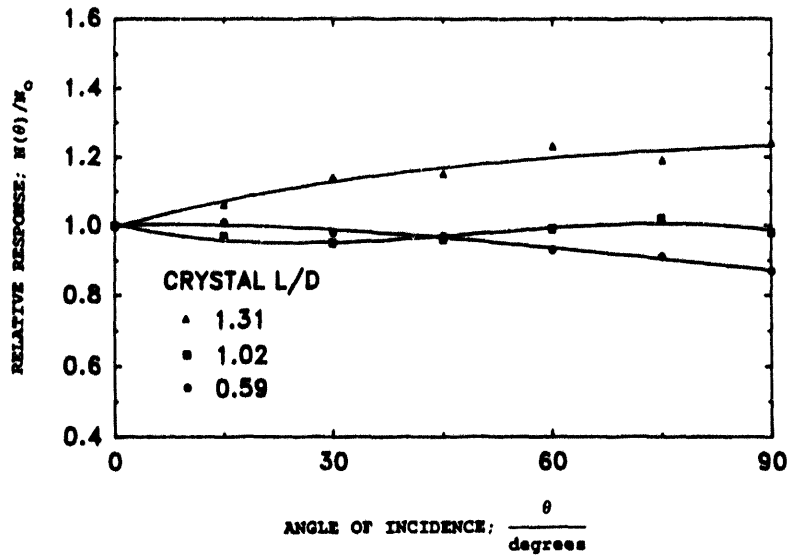


Figure 3.7. Angular response over the range 0-90° at 1408 keV for three length-to-diameter ratios.

The angular correction factor is computed as a weighted average of the normalized detector response as a function of angle, $N(\theta)/N_o$, over the flux angular distribution,

$$\frac{N_f}{N_o} = \frac{1}{\rho} \int_{\theta_1}^{\theta_2} \Phi(\theta) \frac{N(\theta)}{N_o} d\theta \qquad (3.2)$$

For a detector positioned in a half space source geometry, the limits of integration in the above equation would be 0 to $\pi/2$. The sensitivity in the case of measurements over a soil half space is maximized with the detector facing downward, in which case 0° is the perpendicular to the ground plane and normal incidence at the detector face.

Equation 3.2 can be evaluated numerically using the experimental data for $N(\theta)/N_o$ and calculated values of $\phi(\theta)$ for different source energies and geometries.

Figure 3.8 shows the results for three different shape detectors for two different source geometries, a plane source atop the ground and a uniformly distributed source with depth. As explained previously, when the crystal length/diameter ratio is close to 1, a more uniform angular response can be expected and this is also reflected in the behavior of the function $N_f/N_o$. Also, as expected, the angular response tends to flatten out at high energies, but can vary quite a bit at low energies. Although the value of $N_f/N_o$ can be seen to vary considerably for different detectors and as a function of energy for a given detector, there are only minor differences for different source depth distributions. This results from the fact that, at a given energy, the angular distribution of the fluence does not change dramatically with the

source depth profile. This is fortunate in that a large error will not result in the measurement of fluence rate if the source depth profile is not known.

The situation of a detector facing upward with the dewar underneath will result in a lower efficiency for the measurement of radionuclides in soil. The dewar itself will substantially attenuate the photon fluence from the ground underneath and, in general, the detector mounting will result in a lower response at incident angles at the back end of the crystal. However, since the angular distribution of the fluence is peaked toward the horizontal direction, the overall effect is not substantial. The data of Helfer and Miller (1988) indicate that the value of $N_f/N_o$ would only be reduced by a few percent for surface source distributions for detector facing up as compared to facing down. For a uniform source distribution in the soil, the reduction would be typically 10% to 20%.

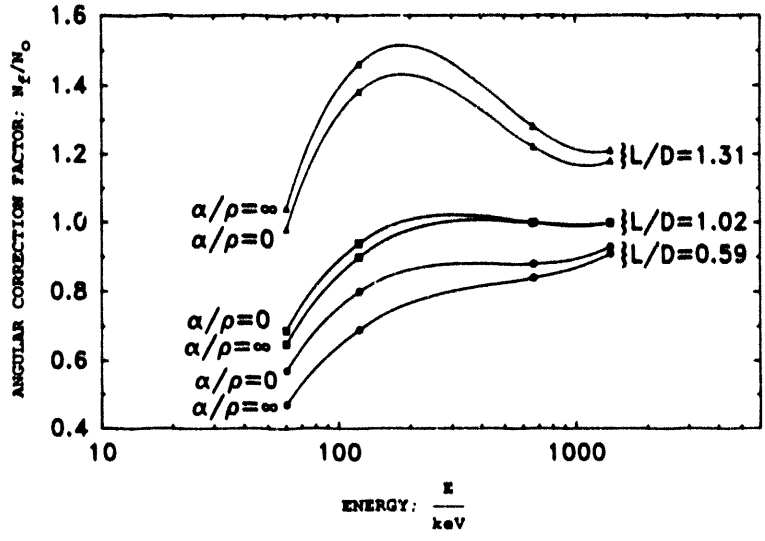


Figure 3.8. Angular correction factor as a function of energy for a plane and uniform source distributions for three different detectors with length-to-diameter ratios as shown.

********

## *EXAMPLE 3*

*Determination of $N_f/N_o$ at One Energy and One Depth Distribution*

*The following peak counts were measured with a $^{137}Cs$ source at a fixed distance of 1.5 m to the Ge crystal center. The relative response (to 0°, normal incidence) was then calculated and appears in the second column.*

| *Angle* | *Peak Counts* | *Relative Response* |
|---|---|---|
| *0* | *13532* | *1.00* |
| *15* | *13436* | *0.99* |
| *30* | *13000* | *0.96* |
| *45* | *12381* | *0.91* |
| *60* | *11828* | *0.87* |
| *75* | *11269* | *0.83* |
| *90* | *10707* | *0.79* |

*These data are plotted below and a smooth curve is drawn:*

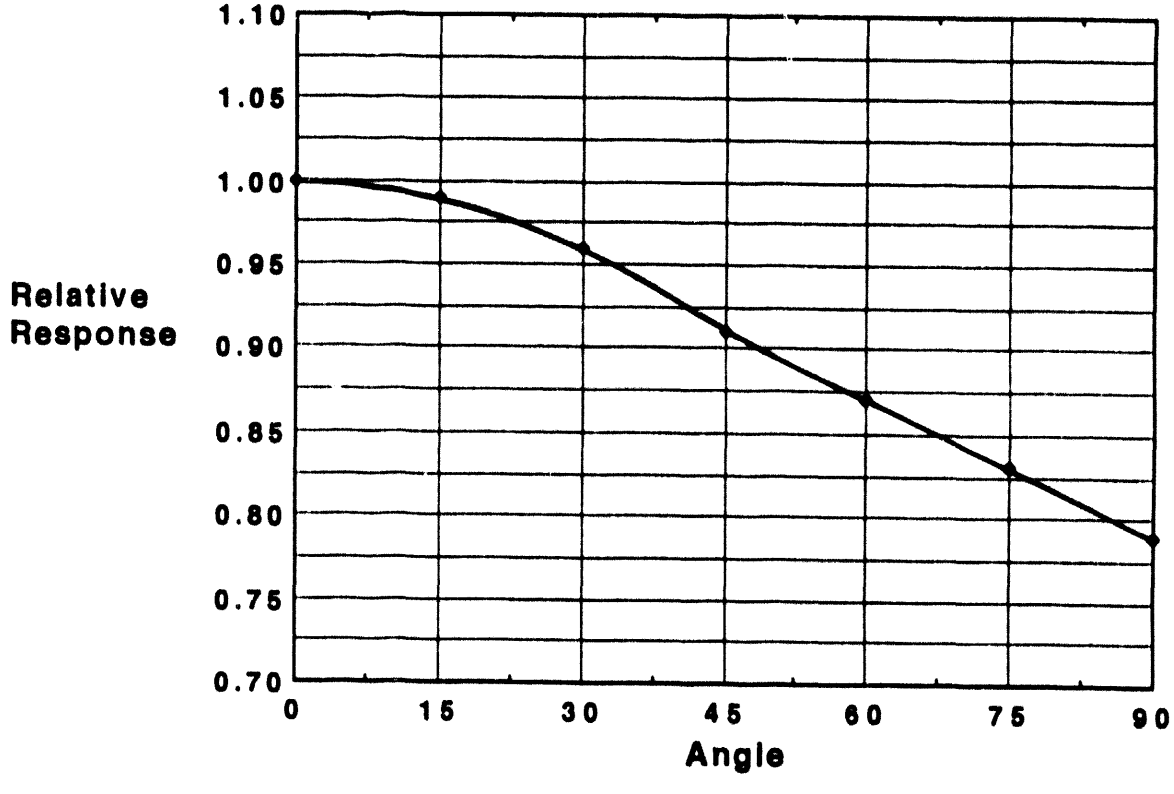

*This detector is to be used in the field facing down. Thus, θ = 0° is normal incidence. To calculate $N_f/N_o$ data on the flux distribution as a function of angle θ is taken from Table 6 in Beck et al. (1972). For each range in angles, the corresponding detector response is taken from the graph above. The following numerical integration is performed*

| θ(°) | Relative Flux | Relative Response | Flux•Response |
|---|---|---|---|
| 0-26 | 0.06 | 0.99 | 0.059 |
| 26-37 | 0.07 | 0.96 | 0.067 |
| 37-46 | 0.07 | 0.93 | 0.065 |
| 46-53 | 0.08 | 0.91 | 0.073 |
| 53-60 | 0.09 | 0.89 | 0.080 |
| 60-66 | 0.09 | 0.86 | 0.077 |
| 66-73 | 0.12 | 0.84 | 0.101 |
| 73-79 | 0.12 | 0.82 | 0.098 |
| 79-84 | 0.15 | 0.81 | 0.122 |
| 84-90 | 0.15 | 0.80 | 0.120 |
| Σ | 1.00 | - | 0.862 |

*The angular correction factor, $N_f/N_o$ for this energy and source distribution is thus 0.86.*

********

********

## *EXAMPLE 4*

*Generation of a Curve for $N_f/N_o$*

*Using the procedure outlined in Example 3, the following values of $N_f/N_o$ were generated for a detector for four different energies and three different source depth distributions:*

| *Energy (keV)* | *$\alpha/\rho = 0$* | *$\alpha/\rho = 0.21$* | *$\alpha/\rho = \infty$* |
|---|---|---|---|
| *60* | *0.57* | *0.54* | *0.47* |
| *122* | *0.81* | *0.77* | *0.69* |
| *662* | *0.89* | *0.86* | *0.83* |
| *1408* | *0.93* | *0.92* | *0.91* |

*These distributions are plotted below and fit with a smooth curve. These curves would then be sufficient to provide the angular correction factor for virtually any situation.*

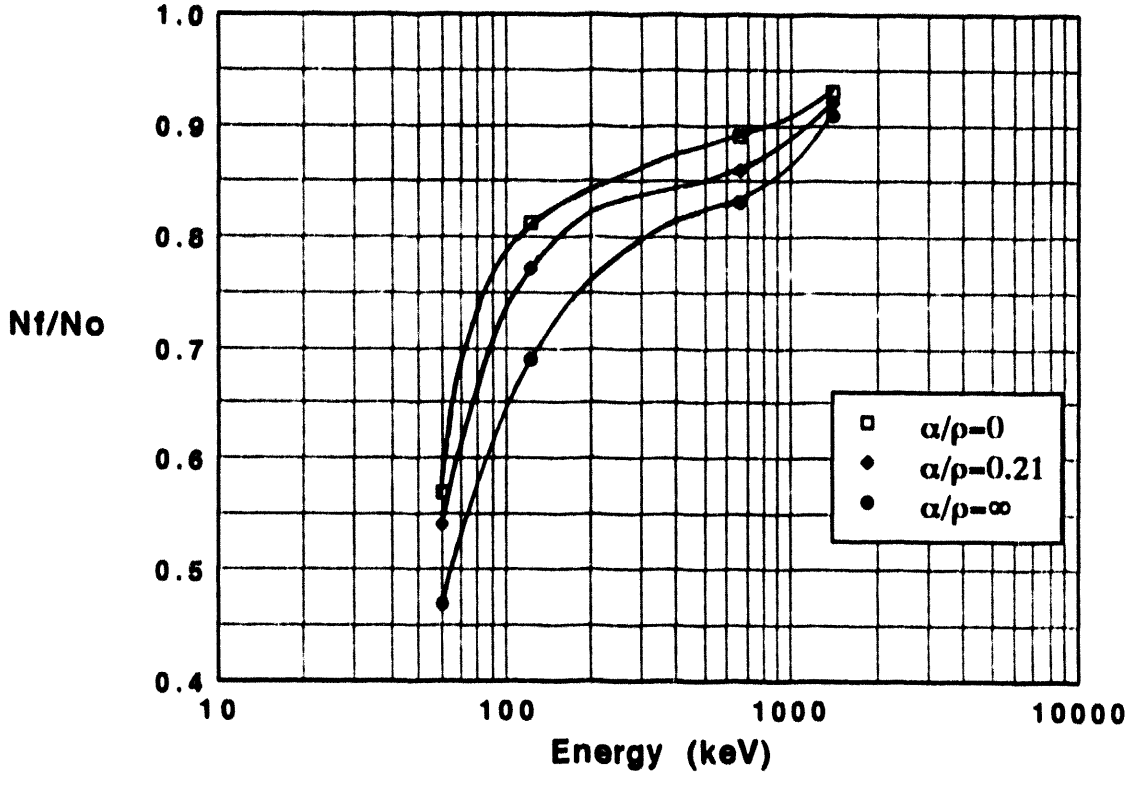


********

## GENERIC CONVERSION FACTORS

In lieu of developing a full calibration for a detector, generic calibration factors can be applied if a high degree of accuracy is not required. These factors were developed on the basis of experimental findings on the response characteristics of a number of different Ge detectors of various sizes and shapes and have been published in Helfer and Miller (1988). The only parameters needed are the manufacturer's quoted efficiency at 1332 keV, the crystal L/D ratio, and the detector orientation in the field (facing up or down). These generic factors are estimated to have an uncertainty of ±10% at energies above 500 keV and ±15% between 200 and 500 keV. Due to the sensitivity of the response at low energies to individual detector characteristics, they cannot be used below 200 keV.

# SECTION 4. INFERRED QUANTITIES

## CONCENTRATION IN SOIL

Having determined the three separate quantities, $N_o/\phi$, $N_f/N_o$, and $\phi/A$, their product yields the desired conversion factor, $N_f/A$. For radionuclides uniformly distributed with depth in the soil ($\alpha/\rho = 0$), the term A is in units of activity per unit mass. As such, there is no need to determine the soil density.

Although the assumption of a uniform profile in the soil for natural emitters is generally safe, unusual situations where there is markedly different soil strata of varying nuclide concentration may produce anomalous results. This situation could arise if landscaping has been performed where topsoil from a different area has been used. Also, evaluations of the $^{238}U$ series must be done with the awareness that $^{222}Rn$ escapes from the soil and that the important gamma-emitting progeny, $^{214}Pb$ and $^{214}Bi$, may not be in equilibrium with $^{226}Ra$ in the soil. In fact, there may be a measurable contribution to the fluence rate at 1 m above the soil from the progeny in the air, particularly under atmospheric inversion conditions. Disequilibrium is also possible for the $^{232}Th$ series due to the exhalation of $^{220}Rn$ (thoron), although this is less likely to be as severe due to its relatively short half-life.

Another effect that may interfere with the interpretation of a spectrum is that of $^{222}Rn$ progeny scavenging during precipitation. In this situation the $^{214}Pb$ and $^{214}Bi$ assume a surface source distribution that can considerably alter the flux and dose rate. For this reason (and to keep people and equipment dry!), it is best to avoid measurements during and for about 2 to 3 hours following rain.

It is possible to consider a fallout product as having a uniform profile if it is deeply distributed or has been mixed through soil cultivation. Depending upon the source gamma energy, plowing to depths of 15 to 30 cm essentially accomplishes this. Although the distribution does not extend to infinity in a situation such as this, in terms of the total gamma flux seen above ground, it is effectively infinite in depth. For *in situ* applications such as this, the concentration that is measured can be considered as representative of the surface soil.

## DEPOSITION/INVENTORY

For radionuclides that are exponentially distributed with depth ($\alpha/\rho > 0$), the term A is in units of activity per unit area. Although the results of analyses of environmental samples are frequently reported in terms of concentration, the fundamental quantity that is of most use for assessing fallout products is the deposition (sometimes referred to as deposition density or inventory). Whereas the deposition remains a constant, the concentration of a fallout product will vary depending upon the depth distribution. To illustrate this point, consider a radionuclide such as $^{137}Cs$ that was deposited in an area 30 years ago from atmospheric nuclear weapons testing. Where the surface soil has retained it, a sample down to 5 cm will yield some concentration, x. On an adjacent strip of land that was plowed deeply, the same sampling protocol will yield a concentration of perhaps only 0.2x. Obviously, this would be a flawed scheme for investigating a potential local source of contamination. Instead, consider a soil core that was taken down to 30 cm. The measured concentration of an aliquot of this sample should be multiplied by the entire sample mass to give the total activity in the core

and then divided by the sample area to give activity per unit area. This would yield the same result for both sites. The only precaution is to sample to a great enough depth to collect essentially all of the deposited activity.

In order to make an accurate assessment of deposited activity with *in situ* spectrometry, an estimate or actual measurement of $\alpha/\rho$ must be made. As such, the time of deposition must be taken into account and assurances that no erosional processes or human activities such as plowing have disturbed the site. For fresh fallout that is dry deposited, the assumption of a surface source ($\alpha/\rho = \infty$) is generally not justified due to the effects of soil surface roughness which effectively buries the source and lowers the fluence at the detector. Wet deposition processes will also tend to distribute the fallout within the surface soil layer such that the assumption of a surface source would not be correct. Experience has shown that a more realistic assumption of $\alpha/\rho$ would be on the order of 1 to 10 $cm^2\ g^{-1}$. Depending upon the degree of uncertainty that is acceptable, experimental determination of the profile may be required via soil sampling. For deposition that occurred in the past, soil sampling is generally required to obtain an accurate value of $\alpha/\rho$. This will be discussed in Section 6.

In making measurements of deposition, one must be aware of the sensitivity of the inferred inventory to the value of $\alpha/\rho$. Figure 4.1 shows an example of the results of a calibration for a 22% efficient Ge detector. The conversion factor, $N_f/A$, is plotted as a function of the source depth constant, $\alpha/\rho$, for the commonly encountered fission product $^{137}Cs$. The conversion factor is seen to change relatively little for values of $\alpha/\rho > 1\ cm^2\ g^{-1}$ (shallow source depth distribution) as compared to values of $\alpha/\rho < 1\ cm^2\ g^{-1}$ (deep source depth distribution). In effect, the error made in inferring the source activity will not be large for a fresh deposition event even if the profile is not precisely known. Conversely, if a measurement of aged fallout is made, accurate results will only be obtained if the profile is determined by some independent means, i.e., soil sampling.

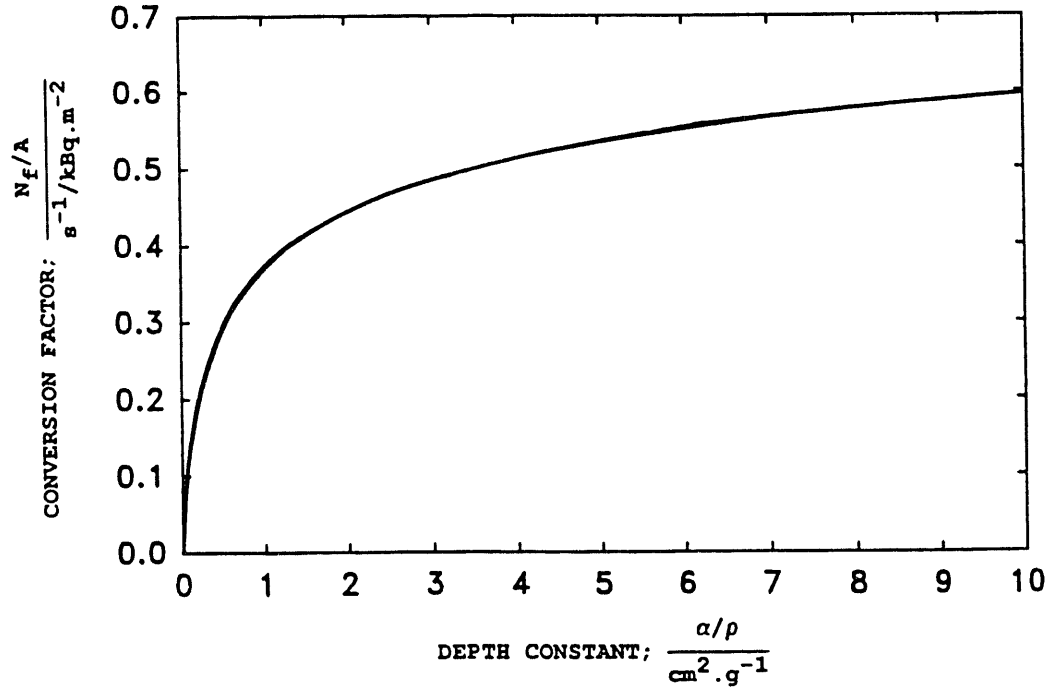


Figure 4.1. Conversion factor $N_f/A$ as a function of the source depth parameter $\alpha/\rho$.

## DOSE RATE IN AIR

One of the most useful quantities that can be determined with *in situ* gamma-ray spectrometry is the dose rate in air (or the exposure rate) for the individual radionuclides present at a site. To do this, the results of transport calculations are used for the infinite half space geometry and the exponential source distribution. The conversion factors, I/A, exposure rate per unit activity in the soil, can be found in Beck et al. (1972) and Beck (1980). One can incorporate these factors directly into the detector calibration using the relationship

$$\frac{N_f}{I} = \frac{N_f/A}{I/A} \tag{4.1}$$

where $N_f/I$ is the full absorption peak count rate per unit exposure rate for that nuclide.

The factor I/A takes into account all of the gamma rays emitted in the decay of that nuclide. Therefore, one does not have to analyze every peak for that nuclide. In practice, however, it is best to analyze more than just one peak, especially if they are well separated in energy to check agreement.

What is not obvious in this analysis is the fact that the derived quantity, $N_f/I$, is less sensitive to $\alpha/\rho$ than is $N_f/A$. This results from the fact that as the source distribution in the soil gets deeper, the primary flux decreases relatively rapidly compared to the scattered component. This scattered component still contributes to the dose rate. To illustrate this, Figure 4.2 compares these to the two calibration factors $N_f/I$ and $N_f/A$ as a function of the relaxation depth, $\alpha^{-1}$, where the soil density = 1.6 g $cm^{-3}$. This range in depth profiles extends from a fresh deposit to one that is perhaps 30 years old. It can be seen that the exposure rate factor varies by only 50% or so whereas the inventory factor varies by about a factor of 7. Thus, only a rough estimate of the depth profile is needed to predict the dose rate. At the same time, substantial errors can be made in the inventory estimate if the wrong depth profile is used.

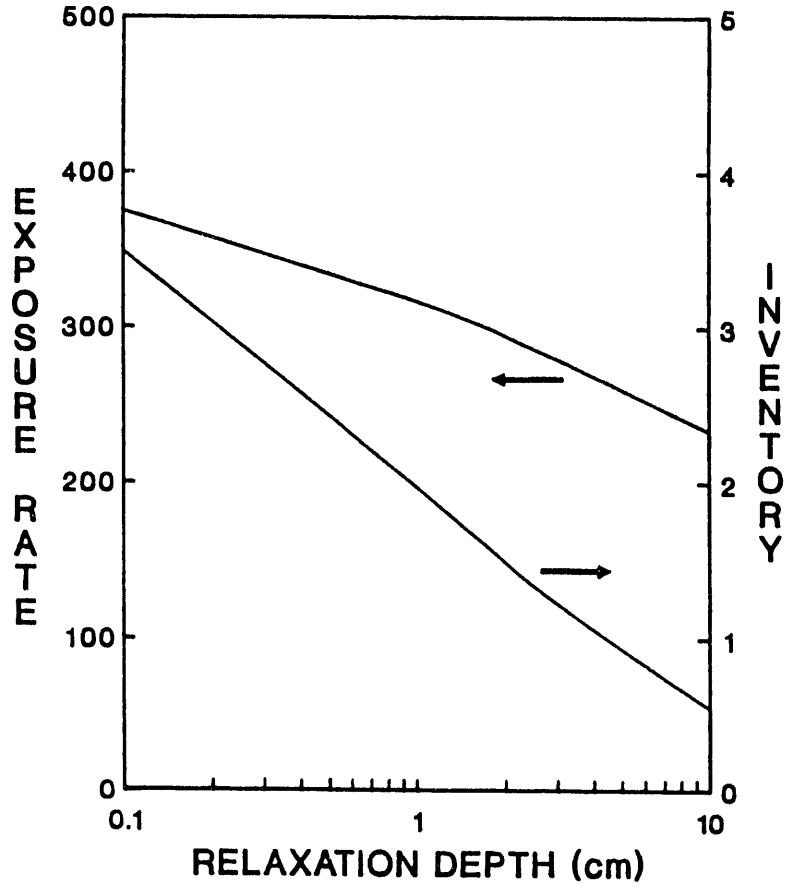


Figure 4.2. Exposure rate and inventory conversion factors as a function of the relaxation length for $^{137}Cs$.

********

## *EXAMPLE 5*

*Computation of $N_f/A$ and $N_f/I$ for One Nuclide at One Energy*

*The factors to convert from peak count rate to the concentration in the soil and to dose rate in air are desired for the 352 line of $^{214}Pb$ ($^{238}U$ series). The detector is the same as in Examples 1-4.*

1. *Determine the flux per unit activity.*

   *Since this is a natural radionuclide, it will be assumed that there is a uniform distribution in the soil. Using Table 1 from Beck et al. (1972) and interpolating from the values in the column for $\alpha/\rho = 0$, the flux at 352 keV is 4.65 $\gamma\ cm^{-2}$ s. This value is per unit gamma emission per gram of soil. If the intensity of this line is 0.366 $\gamma$ per disintegration, then*

   $$\phi/A = 0.366 \times 4.65 = 1.70\ \gamma\ cm^{-2}\ g\ per\ Bq\ g^{-1} = 0.00170\ \gamma\ cm^{-2}\ s^{-1}\ per\ Bq\ kg^{-1}$$

2. *Determine the response at normal incidence per unit flux.*

   *From Example 2, we apply the equation of the fit at 352 keV (0.352 MeV):*

   $$ln(N_o/\phi) = 5.15 - 0.963\ ln(0.352) = 6.155$$

   $$N_o/\phi = e^{6.155} = 471\ counts\ min^{-1}\ per\ \gamma\ cm^{-2}\ s^{-1}$$

3. *Determine the angular correction factor.*

   *Given a uniform profile, we use the graph from Example 4 and see that for $\alpha/\rho = 0$, at 352 keV, $N_f/N_o = 0.87$.*

4. *Compute the product of the three factors.*

   $$N_f/A = \phi/A \times N_o/\phi \times N_f/N_o = 0.00170 \times 471 \times 0.87 = 0.697\ counts\ min^{-1}\ per\ Bq\ kg^{-1}$$

5. *Apply the concentration to dose rate in air conversion factor.*

   *The factor can be found in the conversion table at the back of this report or in Helfer and Miller (1988). This factor takes into account all of the other gamma lines in the $^{238}U$ series and assumes secular equilibrium.*

   $$N_f/I = N_f/A + I/A = 0.697/0.45 = 1.55\ counts\ min^{-1}\ per\ nGy\ h^{-1}$$

********

# SECTION 5. RADIATION SOURCES IN THE ENVIRONMENT

## NATURAL EMITTERS

Virtually any spectrum collected over soil will reveal the presence of the three primordial natural radionuclides, $^{238}U$, $^{232}Th$, and $^{40}K$. In the case of $^{238}U$, detection is made through the analysis of its progeny, principally $^{214}Pb$ and $^{214}Bi$. For $^{232}Th$, the progeny $^{228}Ac$ and $^{208}Tl$ are commonly used. As mentioned previously, these radionuclides are generally distributed uniformly with depth in the soil. As such, the appropriate quantity to report is the concentration, i.e., the specific activity (pCi $g^{-1}$, Bq $kg^{-1}$, etc.). Since these natural radionuclides are likely to contribute substantially to the total gamma flux, the exposure rate or dose rate in air is a useful quantity to report as well. As explained in the following section, the summation of all contributions to the dose rate should be made and compared to a reading from an instrument such as a PIC.

Table 5.1 lists some of the more prominent peaks that are seen in a spectrum and which are the best to analyze. As a standard practice, the conversion factors $N_f/A$ and/or $N_f/I$ should be computed for these lines, as they will almost always be used.

One characteristic of an *in situ* spectrum is that the continuum rises substantially at low energies from the absorption of scattered radiation in the air by the Ge crystal. This makes it difficult to detect and analyze peaks below about 200 keV. For instance, the rather weak 186 keV peak from $^{226}Ra$ superimposed on this large continuum does not usually give highly precise results due to the counting error.

One cosmogenically produced isotope that can sometimes be seen is $^{7}Be$ (478 keV, 53 day half-life). Since it is produced in the atmosphere and deposited on the earth's surface, it can be expected to have an exponential profile like that of a typical fission fallout product. Due to its short half-life, it can also be expected to lie close to the soil surface and thus have a high value of $\alpha/\rho$.

## FALLOUT EMITTERS

Due to nuclear weapons testing in the atmosphere, measurable amounts of the fission product $^{137}Cs$ can be seen in surface soils around the world. Also, many areas, especially in Europe, show the activation product, $^{134}Cs$, along with additional amounts of $^{137}Cs$ from Chernobyl fallout. Other, less intense, and shorter-lived isotopes from Chernobyl, such as $^{125}Sb$ and $^{106}Ru$, can be sometimes seen as well.

For common fallout products such as $^{125}Sb$ and $^{106}Ru$ and for other isotopes that one would expect to encounter, it is useful to determine the conversion factor $N_f/A$ and plot it for several different values of $\alpha/\rho$. A smooth curve can be drawn through the points or a fit can be applied, as shown in Figure 4.1.

For *in situ* applications where there is potential for inhomogeneity in the horizontal distribution of deposited activity due to sparse ground cover, accurate measurements can still be performed providing that the scale of these inhomogeneities is small in comparison to the field of view of the detector. As an example, fallout in semi-arid regions may tend to clump

under scattered plants from the effects of wind blown soil. If the depth distribution of the radionuclides is approximately the same for bare ground, as well as under the plants, no correction is needed as the application of the appropriate conversion factor for that depth distribution will yield the average inventory for that site. However, it is possible that there may be two or more distinct depth profiles associated with the various ground covers in which case separate determinations must be made. The infinite half space in this circumstance can be considered a collection of subspaces, each with its own characteristic radionuclide inventory and depth profile. The conversion factor for field spectrometry is then computed as an average, weighted by the fraction of the total deposited activity associated with each ground cover. An estimate of this can be made through selected soil sampling to determine the inventory and by measuring the fraction of the half space for each ground cover. In a strict sense, the *in situ* spectrum in this situation does not provide an independent measure of the deposited activity in that there is a reliance on the data provided by the soil samples. However, the average conversion factor is bounded by the range in respective values for each type of ground cover. This range may be small compared to the variation in deposition density so that the *in situ* spectrum provides a reasonably accurate average without resorting to far more extensive soil sampling. For more details on this subject, the reader is referred to Miller and Helfer (1985).

## COSMIC RADIATION

A portion of the continuum seen in a Ge spectrum is due to the interaction of cosmic-ray secondary radiation in the crystal. The degree of this contribution can be estimated from the count rate above the 2.615-MeV line from $^{208}$Tl. Generally, it is a small fraction of the count rate due to terrestrial gamma radiation. The overall effect is to increase somewhat the error associated with the analysis of a peak in the spectrum in that the continuum under that peak is slightly higher.

It is important to realize, however, that a measurement of the external dose rate will include a contribution from the cosmic component. Many survey instruments have some response to cosmic radiation. If a comparison is made between a survey instrument reading and the sum of the dose rates inferred from peak analysis with a Ge detector, it must be remembered that the latter provides only the terrestrial gamma component.

In general, the dose rate from cosmic radiation increases towards the earth's poles and decreases toward the equator. For mid-latitudes, Figure 5.1 provides a useful conversion from altitude/pressure to cosmic-ray dose rate. A reading with a pressure meter would be the preferred method with which to infer the cosmic-ray component. In place of this, a geological survey map can be used to find one's altitude. In using this chart, a limitation on its accuracy must be recognized. There are variations of a few percent with the 11-year solar cycle and somewhat smaller variations with season. During periods of maximum solar activity (as measured by sunspots for instance), the cosmic component tends to be lower, while during periods of a "quiet" sun it is higher. The overall uncertainty given both these spatial and temporal variations is estimated to be on the order of 10%.

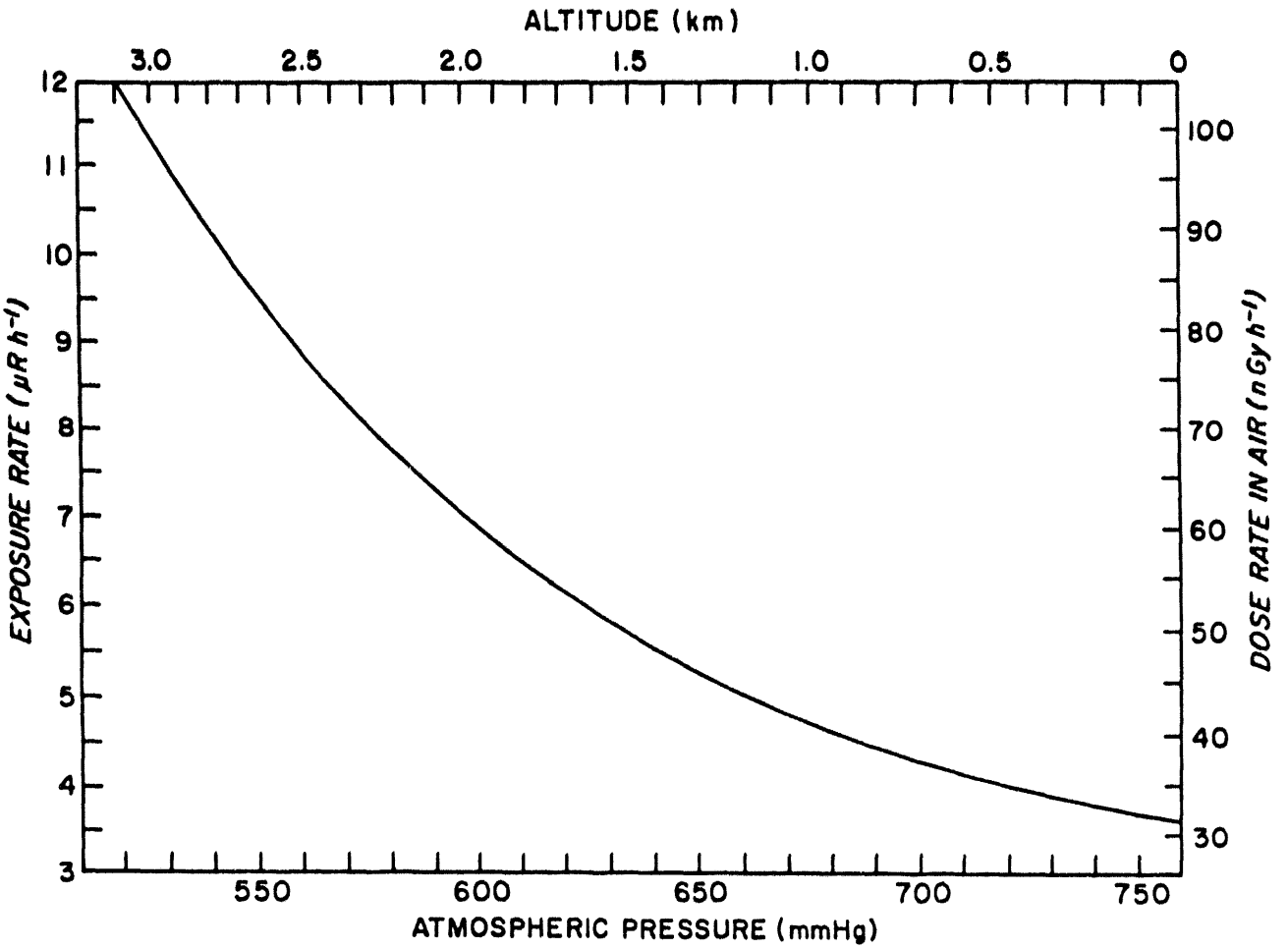


Figure 5.1. Mid-latitude conversion factors for cosmic-ray dose and exposure rate as a function of altitude and atmospheric pressure.

Table 5.1

Principal Gamma Ray Energies for the Analysis of Natural Radionuclides

| Energy (keV) | Nuclide | Parent Series | Comments |
|---|---|---|---|
| 186 | $^{226}Ra$ | $^{238}U$ | low intensity, high continuum, cannot be resolved from $^{235}U$ peak at 185 keV |
| 239 | $^{212}Pb$ | $^{232}Th$ | strong peak, contribution from $^{224}Ra$ peak at 241 keV, interference from $^{214}Pb$ peak at 242 keV |
| 295 | $^{214}Pb$ | $^{238}U$ | generally clean peak, fairly strong |
| 352 | $^{214}Pb$ | $^{238}U$ | generally clean, strong peak |
| 583 | $^{208}Tl$ | $^{232}Th$ | generally clean, strong peak |
| 609 | $^{214}Bi$ | $^{238}U$ | strong peak, interference from 605 keV peak if $^{134}Cs$ is present |
| 911 | $^{228}Ac$ | $^{232}Th$ | generally clean, strong peak |
| 965+969 | $^{228}Ac$ | $^{232}Th$ | doublet, not as strong as 911 peak |
| 1120 | $^{214}Bi$ | $^{238}U$ | reasonably strong, continuum relatively low |
| 1461 | $^{40}K$ | - | clean, strong, only peak for this nuclide |
| 1765 | $^{214}Bi$ | $^{238}U$ | reasonably strong, continuum low |
| 2615 | $^{208}Tl$ | $^{232}Th$ | clean, strong, continuum very low |

# SECTION 6. QUALITY ASSURANCE

## ERROR ESTIMATES

Sources of random and systematic uncertainties for *in situ* spectrometry include deviations in the assumed source geometry parameters, soil density and mass attenuation coefficients, detector parameters, and counting statistics. For the case of a fresh deposition event, the source geometry and soil parameters are not crucial. It is unlikely that errors greater than 10% would result since the source is near the soil surface. For more deeply distributed radionuclides, errors relating to departures from the assumed source geometry and soil medium attenuation are not readily predictable. For this reason, it is important to corroborate estimates of inventory with independent methods such as soil sampling (see below).

Systematic errors relating to detector calibration can be estimated based on the quoted uncertainties of the calibration sources used. These errors would tend to be around 3% or less. Calibration source uncertainty is not a factor for the angular response determination since the measurements are normalized. There is, however, a few percent uncertainty in the application of a value of $N_f/N_o$ due to variations in the angular distribution of the flux with source depth profile and any experimental error in the measurement of angles during the calibration.

One source of error that should be reported and which is easy to estimate is the statistical counting error (sometimes referred to as $\pm$ 1 $\sigma$) for each peak analyzed. Software peak analysis routines generally calculate such an error. If not, a basic estimate is given by the square root of the sum of the peak (net) counts and the gross counts in the region of interest. The relative error would simply be this quantity divided by the peak counts.

As a general quality control practice, the detector calibration should be checked on a regular basis. To do this, the value of $N/\phi$ can be measured at two energies, one high and the other low, and for two angles, normal incidence and sidewall incidence. The detector performance over time should be evaluated as any deterioration in the energy resolution could point to loss in efficiency as well. If the detector is repaired by the manufacturer, a complete recalibration may be necessary, particularly if the crystal has been reworked.

## SOURCE DEPTH PROFILE DETERMINATIONS

In certain *in situ* applications, and particularly for deposited radionuclides that have weathered into the soil, one would like to ascertain the source depth distribution. This can be done by taking soil samples from different depths. One of the easiest ways in which to do this is to hammer a corer (sometimes referred to as a cookie cutter) in to the ground and remove a soil section. If the soil bore hole does not collapse, one can continue the procedure to greater depths with longer corers, taking care not to spill topsoil into the hole. Alternatively, once the corer is in the ground, the area is defined and various depth layers can be carefully spooned out. It is best to take several cores in this manner, and composite the samples. More complete information on soil sampling can be found in the EML Procedures Manual.

Useful depth increments for the determination of $\alpha/\rho$ are 0 - 2.5 cm, 2.5 - 5 cm (or a combined 0 - 5 cm), 5 - 10 cm, 10 -15 cm, and 15 - 30 cm (or a combined 10 - 30 cm). Uniformity of the natural emitters with depth can be checked by counting these samples in a laboratory based shielded detector. Moreover, a plot of the concentration with depth for man-made activity can yield the depth penetration factor $\alpha/\rho$. A convenient method is to compute the total activity in the core (assuming it was of great enough depth to contain all of the deposited activity) and the fraction of the total below a given depth versus that depth. The depth should be in terms of mass per unit area (g $cm^{-2}$), which is simply the original wet mass divided by the area of the corer. A straight-line fit to the data points provides a slope which is just the value of $\alpha/\rho$ ($cm^2$ $g^{-1}$). Figures 6.1 and 6.2 show several examples of depth profiles that were determined in this manner.

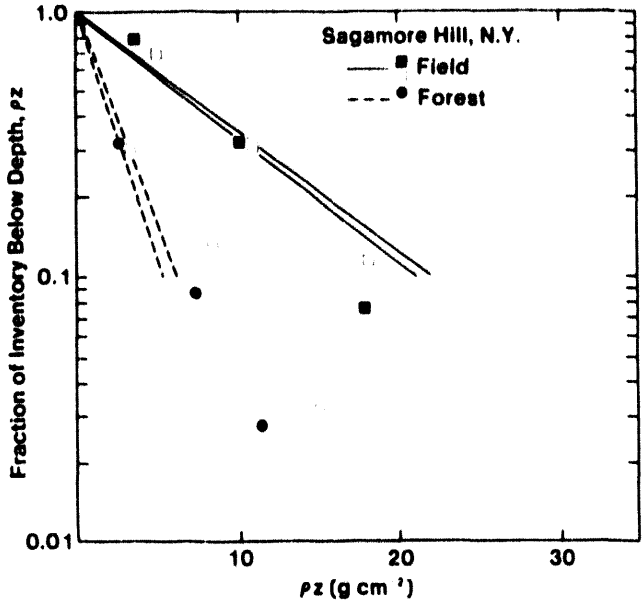


Figure 6.1. Fraction of inventory below mass depth, ρz, over a field and forest location in Sagamore Hill, New York.

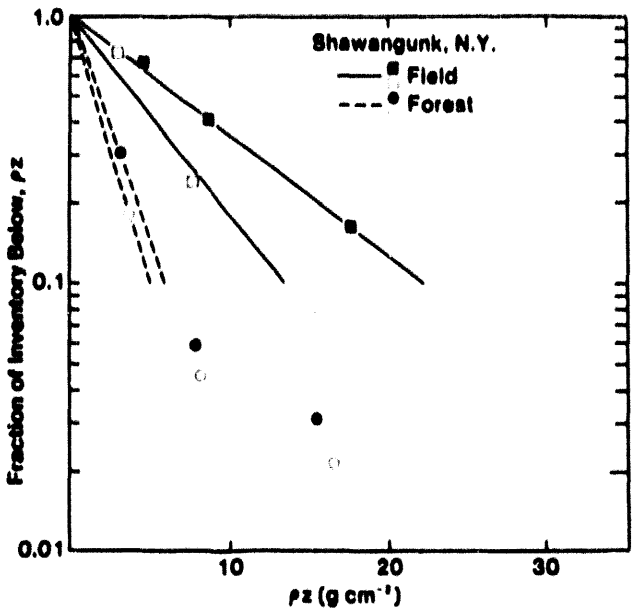


Figure 6.2. Fraction of inventory below mass depth, ρz, over a field and forest location in Shawangunk, New York.

## COMPARISONS TO SOIL SAMPLES

The simplest comparison to make between *in situ* spectrometry and soil sample analysis is a comparison of concentrations for the natural emitters. Some caution is needed here for the $^{238}U$-$^{226}Ra$ series, however, since the emanation of $^{222}Rn$ from either the soil in the field or from the sample complicates matters. Typically, disequilibrium on the order of 10% to 20% can result if the soil is open to the free air. This would be the case for surface soil. For a sample that has been sealed in a container (not porous to radon and with no air space at the top where radon could collect and the progeny could plate out) equilibrium would be achieved in several half-lives, about 3 weeks.

Another factor to consider in the $^{238}U$ series is $^{210}Pb$ (22 year half-life). Since this nuclide follows $^{222}Rn$ in the decay chain, it cannot be expected to be in equilibrium for surface soils. In wet regions, it is likely to have a higher concentration than $^{226}Ra$ and in dry regions, a lower concentration.

An important consideration in making a comparison with soil samples is soil moisture content. Generally, samples are dried before counting. In order to make a valid comparison to *in situ* measurements, it is necessary to weigh the sample wet and correct the dry concentration to wet concentration. This might typically be a 10% to 25% correction.

Comparisons of fallout activity are generally best made in terms of activity per unit area as pointed out before. Due to the potential inhomogeneity in the horizontal distribution of fallout activity, a representative soil sample would generally have to measure several hundred $cm^2$ and be comprised of several cores from different spots.

## COMPARISONS TO TOTAL IONIZATION

One of the best techniques to employ for quality assurance purposes is to make a dose rate comparison between results obtained with the Ge detector and those of another instrument. For instance, the total dose rate in air from penetrating radiation (gamma and cosmic) in the environment can be made fairly accurately with a properly calibrated pressurized ionization chamber. This can be compared with the sum of the dose rates for each nuclide from spectrometric determinations with the cosmic component added in. Agreement to within ±5% is a sign that the detector calibration is good and that the assumed source geometry is correct. Disagreement by more than 10% points to a calibration problem or a radical departure from the assumed source geometry.

## USEFUL CONVERSION FACTORS

Basic Units

$1\ R = 2.58 \times 10^{-4}\ C\ kg^{-1}$

$1\ mCi\ km^{-2} = 37\ Bq\ m^{-2}$

$1\ mCi\ km^{-2} = 1\ nCi\ m^{-2}$

$1\ mCi\ km^{-2} = 0.1\ pCi\ cm^{-2}$

$1\ pCi\ g^{-1} = 2.22\ dpm\ g^{-1}$

$1\ pCi\ g^{-1} = 37\ Bq\ kg^{-1}$

Other Factors

$1\ \mu R\ h^{-1} \rightarrow 8.7\ nGy\ h^{-1}$

for a soil half-space:

$1\ pCi\ g^{-1}$ of $^{238}U$ + progeny $\rightarrow 1.90\ \mu R\ h^{-1}$
$1\ Bq\ kg^{-1}$ of $^{238}U$ + progeny $\rightarrow 0.45\ nGy\ h^{-1}$

$1\ pCi\ g^{-1}$ of $^{232}Th$ + progeny $\rightarrow 2.82\ \mu R\ h^{-1}$
$1\ Bq\ kg^{-1}$ of $^{232}Th$ + progeny $\rightarrow 0.66\ nGy\ h^{-1}$

$1\ pCi\ g^{-1}$ of $^{40}K \rightarrow 0.179\ \mu R\ h^{-1}$
$1\ Bq\ kg^{-1}$ of $^{40}K \rightarrow 0.042\ nGy\ h^{-1}$

## SECTION 7. SUGGESTED READINGS

Publications of EML (HASL)


Beck, H. L.
"Exposure Rate Conversion Factors for Radionuclides Deposited on the Ground"
USDOE Report EML-378 (1980)
*Tables listing the exposure rate per unit deposited activity for over 100 of the most common fission isotopes and over 50 activation products. The conversion factors are given for four different source depth profiles ranging from a recent deposition event to an aged fallout situation.*

Beck, H. L.
"The Physics of Environmental Gamma Radiation Fields"
J. A. S. Adams, W. M. Lowder, and T. F. Gesell (Editors)
In: The Natural Radiation Environment II, CONF-720805-P1, pp. 101-134 (1972)
*A fundamental review of the properties of gamma radiation fields in the environment. Basic flux, exposure rate, and angular distribution data.*

Beck, H. L., J. DeCampo, and C. V. Gogolak
"*In situ* Ge(Li) and NaI(Tl) Gamma-ray Spectrometry"
USDOE Report HASL-258 (1972)
*The "Bible" of in situ gamma spectrometry. A complete description of theory and application with handy reference tables. As useful today as when it was first published.*

Chieco, N. A., D. C. Bogen, and E. O. Knutson (eds.)
"EML Procedures Manual"
USDOE Report HASL-300, 27th edition, Vol. 1, Section 3, February (1992)
*Information on the instrument systems and techniques employed for environmental radiation measurements with emphasis on calibration procedures. Devices covered include Ge and NaI detectors, pressurized ionization chambers, and thermoluminescence dosimeters.*

Helfer, I. K., and K. M. Miller
"Calibration Factors for Ge Detectors Used for Field Spectrometry"
Health Physics 55, 15-29 (1988)
*For those who do not have the time or resources to calibrate their detector, this reference contains equations and tables that provide generic factors based on a manufacturer's quoted specifications for the Ge crystal. Above energies of 500 keV, these factors are estimated to be accurate to within 10%.*

Miller, K. M.
"A Spectral Stripping Method for a Ge Spectrometer Used for Indoor Gamma Exposure Rate Measurements"
USDOE Report EML-419 (1984)
*A more advanced topic for experienced gamma spectroscopists. This technique involves additional experimental determinations of detector response and the application of an unfolding routine. It yields the incident flux spectrum (both primary and scattered) which can then be converted to exposure rate. No knowledge of the source geometry is needed.*

Miller, K. M., and I. K. Helfer
"*In situ* Measurements of $^{137}Cs$ Inventory in Natural Terrain"
in: Environmental Radiation '85, Proceedings of the Eighteenth Midyear Topical Symposium of the Health Physics Society, pp. 243-251 (1985)

*The basic approach is described for making measurements at sites with sparse ground cover where fallout was deposited many years ago and where it is likely to have been redistributed by wind and water erosion.*

DATE
FILMED
1/31/94
END